

The Kolmogorov Superposition Theorem can Break the Curse of Dimension When Approximating High Dimensional Functions

Ming-Jun Lai ^{*} Zhaiming Shen[†]

December 29, 2022

Abstract

We explain how to use Kolmogorov Superposition Theorem (KST) to break the curse of dimension when approximating continuous multivariate functions. We first show that there is a class of functions called K -Lipschitz continuous and can be approximated by a ReLU neural network of two layers to have an approximation order $O(d^2/n)$, and then we introduce the K -modulus of continuity of multivariate functions and derive the approximation rate for any continuous function $f \in C([0, 1]^d)$ based on KST. Next we introduce KB-splines by using uniform B-splines to replace the K -outer function and their smooth version called LKB-splines to approximate high dimensional functions. Our numerical evidence shows that the curse of dimension is broken in the following sense. When using the standard discrete least squares method (DLS) to approximate a continuous function f over $[0, 1]^d$, one expects to use a dense data set P , a large number of data locations and function values over the locations. Based on the LKB splines, the structure of K -inner functions leads to a sparse solution of the linear system associated with the DLS. Furthermore, there exists a magic set of points from P with much small in size such that the rooted mean squares error (RMSE) from the DLS based on the magic set is similar to the RMSE of the DLS based on the original set P . In addition, the number of LKB-splines used for approximation is the same as the size of the magic data set. Hence we not need a lot of basis functions and a lot of data locations and function values to approximate a high dimensional continuous function f when f is not very oscillated.

Math. Subject Classification: 41A15, 41A63, 15A23

1 Introduction

Recently, deep learning algorithms have shown a great success in many fronts of research, from image analysis, audio analysis, biological data analysis, to name a few. Incredibly, after a deep learning training of thousands of images, a computer can tell if a given image is a cat, or a dog, or neither of them with very reasonable accuracy. In addition, there are plenty of successful stories such that deep learning algorithms can sharpen, denoise, enhance an image after an intensive training. See, e.g. [22] and [49]. The 3D structure of a DNA can be predicted very accurately by using the DL approach. The main ingredient in DL algorithms is the neural network approximation based on ReLU functions. We refer to [10] and [12] for detailed explanation of the neural network approximation in deep learning algorithms.

^{*}mjlai@uga.edu. Department of Mathematics, University of Georgia, Athens, GA 30602. This author is supported by the Simons Foundation Collaboration Grant #864439.

[†]Department of Mathematics, University of Georgia, Athens, GA 30602.

Learning a multi-dimensional data set is like approximating a multivariate function. The computation of a good approximation suffers from the curse of dimension. For example, suppose that $f \in C([0, 1]^d)$ with $d \gg 1$. One usually uses Weierstrass theorem to have a polynomial P_f of degree n such that

$$\|f - P_f\|_\infty \leq \epsilon$$

for any given tolerance $\epsilon > 0$. As the dimension of polynomial space $= \binom{n+d}{n} \approx n^d$ when $n > d$, one will need at least $N = O(n^d)$ data points in $[0, 1]^d$ to distinguish different polynomials in \mathbb{P}_n and hence, to determine this P_f . Notice that many good approximation schemes enable P_f to approximate f at the rate of $O((1/n)^m)$ if f is of m times differentiable. In terms of the number N of data points which should be greater than or equal to the dimension of polynomial space \mathbb{P}_n , i.e. $N \geq n^d$, the order of approximation is $O(1/(N^{1/d})^m)$. When $d \gg 1$ is bigger, the order of approximation is less. This phenomenon is the so-called curse of dimension. Sometimes, such a computation is also called intractable. Similarly, if one uses a tensor product of B-spline functions to approximate $f \in C([0, 1]^d)$, one needs to subdivide the $[0, 1]^d$ into n^d small subcubes by hyperplanes parallel to the axis planes. As over each small subcube, the spline approximation S_f of f is a polynomial of degree k , e.g., $k = 3$ if the tensor product of cubic splines are used. Even with the smoothness, one needs $N = O(k^d)$ data points and function values at these data points in order to determine a polynomial piece of S_f over each subcube. Hence, over all subcubes, one needs $O(n^d k^d)$. It is known that the order of approximation of S_f is $O(1/n^{k+1})$ if f is of $k + 1$ times coordinatewise differentiable. In terms of $N = O(n^d k^d)$ points over $[0, 1]^d$, the approximation order of S_f will be $O(k^{k+1}/N^{(k+1)/d})$. More precisely, in [11], the researchers showed that the approximation order $O(1/N^{1/d})$ can not be improved for smooth functions in Sobolev space $W^{k,p}$ with L_p norm ≤ 1 . In other words, the approximation problem by using the polynomials or by tensor product B-splines is intractable.

Furthermore, many researchers have worked on using ridge functions, neural networks, and ReLU activation functions to approximate multidimensional functions. The orders of all these approximations in L_2 and in L_∞ norms show the curse of dimensionality. See [48], [57], [58], [3] for detailed statements and proofs. That is, the approximation problem by using the neural networks is intractable. However, there is a way to break the curse of dimensionality by using the probability approach. In [4], the following result was established.

Theorem 1 (Barron, 1993) *For every function f in $\Gamma_{B,C}$, every sigmoidal function ϕ , every probability measure μ , and every $n \geq 1$, there exists a linear combination of sigmoidal functions $f_n(x)$, a shallow neural network, such that*

$$\int_B (f(\mathbf{x}) - f_n(\mathbf{x}))^2 d\mu(\mathbf{x}) \leq \frac{(2C)^2}{n}.$$

The coefficients of the linear combination in f_n may be restricted to satisfy $\sum_{k=1}^n |c_k| \leq 2C$, and $c_0 = f(0)$.

Here $\Gamma_{B,C}$ is the class of functions f defined over $B = \{\mathbf{x} \in \mathbb{R}^d, \|\mathbf{x}\| \leq 1\}$ such that $C_f \leq C$, where C_f is defined as follows:

$$C_f = \int_{\mathbb{R}^d} |\omega| |\tilde{f}(\omega)| d\omega$$

with $|\omega| = (\omega \cdot \omega)^{1/2}$ and \tilde{f} is the Fourier transform of f . Note that the order of convergence is independent of the dimension in the L_2 norm sense! This work leads to many recent studies on the properties and structures of Barron space $\Gamma_{B,C}$ and its extensions, e.g. the spectral Barron spaces and the generalization using ReLU functions instead of sigmoidal functions above, see, e.g. [33], [14], [15], [16], [17], [62], [65], and the references therein.

In this paper, we turn our attention to Kolmogorov superposition theorem (KST) and will see how it plays a role in the study of the rate of approximation for neural network computation in deep learning algorithms, how it can break the curse of dimension when approximating high dimensional functions over \mathbb{R}^d for $d = 2$ and $d = 3$, and how it can potentially overcome the curse of dimension when $d \geq 4$. For convenience, we will use KST to stand for Kolmogorov superposition theorem for the rest of the paper. Let us start with the statement of KST using the version of G. G. Lorentz from [46] and [47].

Theorem 2 (Kolmogorov Superposition Theorem) *There exist irrational numbers $0 < \lambda_p \leq 1$ for $p = 1, \dots, d$ and strictly increasing $Lip(\alpha)$ functions $\phi_q(x)$ (independent of f) with $\alpha = \log_{10} 2$ defined on $I = [0, 1]$ for $q = 0, \dots, 2d$ such that for every continuous function f defined on $[0, 1]^d$, there exists a continuous function $g(u)$, $u \in [0, d]$ such that*

$$f(x_1, \dots, x_d) = \sum_{q=0}^{2d} g\left(\sum_{i=1}^d \lambda_i \phi_q(x_i)\right). \quad (1)$$

Note that $\phi_q, q = 0, \dots, 2d$ are called K-inner functions or K-base functions while g is called K-outer function. In the original version of KST (cf. [34] and [35]), there are $2d + 1$ K-outer functions and $d(2d + 1)$ inner functions. G. G. Lorentz simplified the construction to have one K-outer function and $2d + 1$ inner functions with d irrational numbers λ_i . It is known that $2d + 1$ can not be smaller (cf. [13]) and the smoothness of the K-inner functions in the original version of the KST can be improved to be Lipschitz continuous (cf. [18]) while the continuity of ϕ_q in the Lorentz version can be improved to be Lip_α for any $\alpha \in (0, 1)$ as pointed out in [47] at the end of the chapter. There were Sprecher's constructive proofs (cf. [67, 68, 69, 70, 71, 72, 73, 74]) which were finally correctly established in [5] and [6]. An excellent explanation of the history on the KST can be found in [55] together with a constructive proof similar to the Lorentz construction.

Recently, KST has been extended to unbounded domain in [43] and has been actively studied during the development of the neural network computing (cf. e.g. [9], [50], [57], [53]) as well as during the fast growth period of the deep learning computation recently. Hecht-Nielsen [28] is among the first to explain how to use the KST as a feed forward neural network in 1987. In particular, Igel'nik and Parikh [30] in 2003 proposed an algorithm of the neural network using spline functions to approximate both the inner functions and outer function g .

It is easy to see that the formulation of the KST is similar to the structure of a neural network where the K-inner and K-outer functions can be thought as two hidden layers when approximating a continuous function f . However, one of the main obstacles is that the K-outer function g depends on f and furthermore, g can vary wildly even if f is smooth as explained in [21]. Schmidt-Hieber [60] used a version of KST in [5] and approximated the K-inner functions by using a neural network of multiple layers to form a deep learning approach for approximating any Hölder continuous functions. Montanelli and Yang in [53] used very deep neural networks to approximate the K-inner and K-outer functions to obtain the approximation rate $O(n^{-\frac{1}{\log d}})$ for a function f in the class $K_C([0, 1]^d)$ (see [53] for detail). That is, the curse of dimensionality is lessened. To the best of our knowledge, the approximation bounds in the existing work for general function still suffer the curse of dimensionality unless f has a simple K-outer function g as explained in this paper, and how to characterize the class of functions which has moderate K-outer functions is still an open problem.

The development of the neural networks obtains a great speed-up by using the ReLU function instead of a sigmoidal activation function. Sonoda and Murata [66] showed that the ReLU is an approximator and established the universal approximation theorem, i.e. Theorem 3 below. Chen in [8] pointed out that the computation of layers in the deep learning algorithm based on ReLU is a

linear spline and studied the upper bound on the number of knots needed for computation. Motivated by the work from [8], Hansson and Olsson in [27] continued the study and gave another justification for the two layers of deep learning are a combination of linear spline and used Tensorflow to train a deep learning machine for approximating the well-known Runge function using a few knots. There are several dissertations written on the study of the KST for the neural networks and data/image classification. See [7], [5], [19], [44], and etc..

In this paper, we propose to use KST to study the rate of approximation for ReLU neural network computation. The subsequent sections in the paper are structured as follows. In section 2, we explain how to use KST to break the curse of dimension for multivariate continuous functions. That is, we show that the approximation by using the neural networks can be tractable for some classes of functions. We also establish the approximation result for any continuous function based on the modulus of continuity of the K-outer function. In section 3, we introduce KB-splines and LKB-splines which are a smoothed version of KST. We will show that KB-splines are indeed the bases for functions in $C([0, 1]^d)$. In section 4, we numerically demonstrate that LKB-splines are dense in $C([0, 1]^d)$, and because of the KST, more precisely, the structure of K-inner functions, there is a sparse solution using a few number of LKB splines to approximate a continuous function reasonably well. Furthermore, we provide a computational strategy based on matrix cross approximation. This leads to the new concept of magic point set from any dense point set P over $[0, 1]^d$ such that the discrete least squares (DLS) fitting based on the magic point set has the similar rooted mean squares error to the DLS fitting based on the original data set P . As the size of the magic set is much smaller than the size of P , one can approximate any continuous function using its function values over the magic point set and hence, one is able to break the curse of dimension. Numerical evidence will be provided for 2D and 3D settings to show that the DLS based on the magic point sets can well approximate continuous, not very oscillating functions.

2 ReLU Network Approximation via KST

We will use σ_1 to denote ReLU function through the rest of discussion. It is easy to see that one can use linear splines to approximate K-inner (continuous and monotone increasing) functions $\phi_q, q = 0, \dots, 2d$ and also approximate the K-outer (continuous) function g . We refer to Theorem 20.2 in [59]. On the other hand, we can easily see that any linear spline function can be written in terms of linear combination of ReLU functions and vice versa, see, e.g. [10], and [12]. (We shall include another proof later in this paper.) Hence, we have

$$L_q(t) := \sum_{j=1}^{N_q} c_{q,j} \sigma_1(t - y_{qj}) \approx \phi_q(t)$$

for $q = 0, \dots, 2d$ and

$$S_g(t) := \sum_{k=1}^{N_g} w_k \sigma_1(t - y_k) \approx g,$$

where g is the K-outer function of a continuous function f . Based on KST and the universal approximation theorem (cf. [9], [29], [57]), it follows that

Theorem 3 (Universal Approximation Theorem (cf. [66])) *Suppose that $f \in C([0, 1]^d)$ is a continuous function. For any given $\epsilon > 0$, there exist coefficients $w_k, k = 1, \dots, N_g$, $y_k \in [0, d], k =$*

$1, \dots, N_g, c_{q,j}, j = 1, \dots, N_i$ and $y_{q,j} \in [0, 1], j = 1, \dots, N_i$ such that

$$|f(x_1, \dots, x_d) - \sum_{q=0}^{2d} \sum_{k=1}^{N_g} w_k \sigma_1 \left(\sum_{i=1}^d \lambda_i \sum_{j=1}^{N_q} c_{q,j} \sigma(x_i - y_{qj}) - y_k \right)| \leq \epsilon. \quad (2)$$

In fact, many results similar to the above (2) have been established using other activation functions (cf. [9], [36], [53], and etc.).

For each continuous function $f \in C([0, 1]^d)$, let g_f be the K-outer function associated with f . Let

$$K_C = \{f : \text{K-outer function } g_f \text{ is Lipschitz continuous with Lipschitz constant } \leq C\} \quad (3)$$

be the class of K-Lipschitz continuous functions with K-Lipschitz constant C . Note that when f is a constant, its K-outer function $g = \frac{1}{d+1}f$ is also constant (cf. [7]) and hence, is Lipschitz with $C \leq 1$. That is, K_1 is not empty. On the other hand, we can use any univariate Lipschitz continuous function g with Lipschitz constant $\leq C$, e.g. $g(t) = \sin(t)$ over $[0, d]$ to define a multivariate function f by using the formula (1) of KST. Thus the newly defined f is continuous over $[0, 1]^d$ and is belong to (3) with $C = 1$. Any function in K_C is called K-Lipschitz continuous function in this paper. Note that by Theorem 3 the function class K_C is dense in $C([0, 1]^d)$ when $C \rightarrow \infty$.

Note that the neural network being used for approximation in equation (2) is a special class of neural network with two hidden layers of widths $(2d + 1)N_q$ and N_g respectively. Let us call this special class of neural networks the Kolmogorov network, or K-network in short. Let us use $\mathcal{K}_{m,n}$ to denote the K-network of two layers with widths $(2d + 1)m$ and n based on ReLU activation function, i.e.,

$$\mathcal{K}_{m,n}(\sigma_1) = \left\{ \sum_{q=0}^{2d} \sum_{k=1}^n w_k \sigma_1 \left(\sum_{i=1}^d \sum_{j=1}^m c_{qj} \sigma_1(x_i - y_{qj}) - y_k \right), w_k, c_{qj} \in \mathbb{R}, y_k \in [0, d], y_{qj} \in [0, 1] \right\}. \quad (4)$$

Moreover, we use $\mathcal{N}_{m,n}$ to denote the standard ReLU neural network of two hidden layers with widths m and n , i.e.,

$$\mathcal{N}_{m,n}(\sigma_1) = \left\{ \sum_{k=1}^n w_k \sigma_1 \left(\sum_{j=1}^m c_j \sigma_1(\mathbf{w}_j^\top \mathbf{x} - y_j) - z_k \right) : w_k, c_j, z_k, y_j \in \mathbb{R}, \mathbf{w}_j \in \mathbb{R}^d \right\}. \quad (5)$$

It is easy to see that $\mathcal{K}_{m,n} \subset \mathcal{N}_{(2d+1)dm,n}$.

We are now ready to state one of the main results in this paper.

Theorem 4 *We have*

$$\sup_{f \in K_C} \inf_{s \in \mathcal{K}_{n,n}(\sigma_1)} \|f - s\|_{C([0,1]^d)} \leq \frac{C(2d+1)^2}{n}. \quad (6)$$

That is, the order of approximation in (6) shows that the curse of dimension can be broken. In other words, the computation becomes tractable. The above result improved the similar one in [53]. Also, the researchers in [54] showed that the KST can break the curse of dimension for band-limited functions. Our result breaks the curse of dimensionality for a different class of functions. On the other hand, many researchers used the smoothness of f to characterize the approximation of ReLU neural networks. See [79], [45] and [80], where the approximation rate on the right-hand side of (6) is $O(1/n^{s/d})$ with s being the smoothness of the function f . Their approximation rates suffer from the curse of dimension. In terms of the smoothness of the K-outer function, our result above is believed

to be the correct rate of convergence. In addition, we shall extend the argument to the setting of K-Hölder continuous functions and present the convergence in terms of K-modulus of smoothness.

To prove Theorem 4, we will need some preparations. Let us begin with the space $\mathcal{N}(\sigma_1) = \text{span}\{\sigma_1(\mathbf{w}^\top \mathbf{x} - b), b \in \mathbb{R}, \mathbf{w} \in \mathbb{R}^d\}$ which is the space of shallow networks of ReLU functions. It is easy to see that all linear polynomials over \mathbb{R}^d are in $\mathcal{N}(\sigma_1)$. The following result is known (cf. e.g. [10]). For self-containedness, we include a different proof.

Lemma 1 *For any linear polynomial s over \mathbb{R}^d , there exist coefficients $c_i \in \mathbb{R}$, bias $t_i \in \mathbb{R}$ and weights $\mathbf{w}_i \in \mathbb{R}^d$ such that*

$$s(\mathbf{x}) = \sum_{i=1}^n c_i \sigma_1(\mathbf{w}_i \cdot \mathbf{x} + t_i), \forall \mathbf{x} \in [0, 1]^d. \quad (7)$$

That is, $s \in \mathcal{N}(\sigma_1)$.

Proof. It is easy to see that a linear polynomial x can be exactly reproduced by using the ReLU functions. For example,

$$x = \sigma_1(x), \forall x \in [0, 1]. \quad (8)$$

Hence, any component x_j of $\mathbf{x} \in \mathbb{R}^d$ can be written in terms of (7). Indeed, choosing $\mathbf{w}_i = \mathbf{e}_j$, from (8), we have

$$x_j = \sigma_1(\mathbf{e}_j \cdot \mathbf{x}), \quad \mathbf{x} \in [0, 1]^d, j = 1, \dots, d.$$

Next we claim a constant 1 is in $\mathbb{N}(\sigma_1)$. Indeed, given a partition $\mathcal{P}_n = \{a = x_0 < x_1 < \dots < x_n = b\}$ of interval $[a, b]$, let

$$h_0(x) = \begin{cases} \frac{x - x_1}{x_0 - x_1} & x \in [x_0, x_1] \\ 0 & x \in [x_1, x_n] \end{cases}, \quad (9)$$

$$h_i(x) = \begin{cases} \frac{x - x_{i-1}}{x_i - x_{i-1}} & x \in [x_{i-1}, x_i] \\ \frac{x - x_{i+1}}{x_i - x_{i+1}} & x \in [x_i, x_{i+1}] \\ 0 & x \notin [x_{i-1}, x_{i+1}] \end{cases}, \quad i = 1, \dots, n-1 \quad (10)$$

$$h_n(x) = \begin{cases} \frac{x - x_{n-1}}{x_n - x_{n-1}} & x \in [x_{n-1}, x_n] \\ 0 & x \in [x_0, x_{n-1}] \end{cases}. \quad (11)$$

be a set of piecewise linear spline functions over \mathcal{P}_n . Then we know $S_1^0(\mathcal{P}_n) = \text{span}\{h_i, i = 0, \dots, n\}$ is a linear spline space. It is well-known that $1 = \sum_{i=0}^n h_i(x)$. Now we note the following formula:

$$h_i(x) = \frac{\sigma_1(x - x_{i-1})}{(x_i - x_{i-1})} + w_i \sigma_1(x - x_i) + \frac{\sigma_1(x - x_{i+1})}{(x_{i+1} - x_i)}, \quad (12)$$

where $w_i = -1/(x_i - x_{i-1}) - 1/(x_{i+1} - x_i)$. It follows that any spline function in $S_1^0(\mathcal{P}_n)$ can be written in terms of ReLU functions. In particular, we can write $1 = \sum_{i=0}^n h_i(x) = \sum_{i=0}^n c_i^0 \sigma_1(x - x_i)$ by using (12).

Hence, for any linear polynomial $s(\mathbf{x}) = a + \sum_{j=1}^d c_j x_j$, we have

$$s(\mathbf{x}) = a \sum_{i=0}^n c_i^0 \sigma_1(x - x_i) + \sum_{i=1}^d c_i \sigma_1(\mathbf{e}_j \cdot \mathbf{x}) \in \mathbb{N}(\sigma_1).$$

This completes the proof. \square

The above result shows that any linear spline is in the ReLU neural networks. Also, any ReLU neural network in \mathbb{R}^1 is a linear spline. We are now ready to prove Theorem 4. We begin with the standard modulus of continuity. For any continuous function $g \in C[0, d]$, we define the modulus of continuity of g by

$$\omega(g, h) = \max_{\substack{x \in [0, d] \\ 0 < t \leq h}} |g(x+t) - g(x)| \quad (13)$$

for any $h > 0$. To prove the result in Theorem 4, we need to recall some basic properties of linear splines (cf. [61]). The following result was established in [59].

Theorem 5 *For any function in $f \in C[a, b]$, there exists a linear spline $S_f \in S_1^0(\Delta)$ such that*

$$\|f - S_f\|_{\infty, [a, b]} \leq \omega(f, |\Delta|) \quad (14)$$

where $S_1^0(\Delta)$ is the space of all continuous linear splines over the partition $\Delta = \{a = t_0 < t_1 < \dots < t_n = b\}$ with $|\Delta| = \max_i |t_i - t_{i-1}|$.

In order to know the rate of convergence, we need to introduce the class of function of bounded variation. We say a function f is of bounded variation over $[a, b]$ if

$$\sup_{\forall a = x_0 < x_1 < \dots < x_n = b} \sum_{i=1}^n |f(x_i) - f(x_{i-1})| < \infty$$

We let $V_a^b(f)$ be the value above when f is of bounded variation. The following result is known (cf. [61])

Theorem 6 *Suppose that f is of bounded variation over $[a, b]$. For any $n \geq 1$, there exists a partition Δ with n knots such that*

$$\text{dist}(f, S_1^0(\Delta))_{\infty} = \inf_{s \in S_1^0(\Delta)} \|f - s\|_{\infty} \leq \frac{V_a^b(f)}{n+1}.$$

Let $L = \{f \in C([0, 1]^d) : |f(\mathbf{x}) - f(\mathbf{y})| \leq L_f |\mathbf{x} - \mathbf{y}|, \forall \mathbf{x}, \mathbf{y} \in [0, 1]^d\}$ be the class of Lipschitz continuous functions. We can further establish

Theorem 7 *Suppose that f is Lipschitz continuous over $[a, b]$ with Lipschitz constant L_f . For any $n \geq 1$, there exists a partition Δ with n interior knots such that*

$$\text{dist}(f, S_1^0(\Delta))_{\infty} \leq \frac{L_f(b-a)}{2(n+1)}.$$

Proof. We use a linear interpolatory spline S_f . Then for $x \in [x_i, x_{i+1}]$,

$$\begin{aligned} f(x) - S_f(x) &= f(x) - f(x_i) \frac{x_{i+1} - x}{x_{i+1} - x_i} - f(x_{i+1}) \frac{x - x_i}{x_{i+1} - x_i} \\ &= \frac{(x_{i+1} - x)(f(x) - f(x_i))}{x_{i+1} - x_i} + \frac{(x - x_i)(f(x) - f(x_{i+1}))}{x_{i+1} - x_i} \\ &\leq L_f \frac{(x - x_i)(x_{i+1} - x)}{x_{i+1} - x_i} + L_f \frac{(x_{i+1} - x)(x - x_i)}{x_{i+1} - x_i} \leq \frac{L_f}{2} (x_{i+1} - x_i). \end{aligned}$$

Hence, $|f(x) - S_f(x)| \leq L_f(b-a)/(2(n+1))$ if $x_{i+1} - x_i = (b-a)/(n+1)$. This completes the proof. \square

Furthermore, if f is Lipschitz continuous, so is the linear interpolatory spline S_f . In fact, we have

$$|S_f(x) - S_f(y)| \leq 2L_f|x - y|. \quad (15)$$

We are now ready to prove one of our main results in this paper.

Proof.[of Theorems 4] Since ϕ_q are univariate increasing functions mapping from $[0, 1]$ to $[0, 1]$, they are bounded variation with $V_0^1(\phi_q) \leq 1$. By Theorem 6, there are linear spline functions L_q such that $|L_q(t) - \phi_q(t)| \leq 1/(n + 1)$ for $q = 0, \dots, 2d$.

For K-outer function g , when g is Lipschitz continuous, there is a linear spline S_g with dn distinct interior knots over $[0, d]$ such that

$$\sup_{t \in [0, d]} |g(t) - S_g(t)| \leq \frac{dC_g}{2(nd + 1)} \leq \frac{C_g}{2n},$$

where C_g is the Lipschitz constant of g by using Theorem 7. Now we first have

$$|f(\mathbf{x}) - \sum_{q=0}^{2d} S_g(\sum_{i=1}^d \lambda_i \phi_q(x_i))| \leq \sum_{q=0}^{2d} |g(\sum_{i=1}^d \lambda_i \phi_q(x_i)) - S_g(\sum_{i=1}^d \lambda_i \phi_q(x_i))| \leq \frac{(2d + 1)C_g}{2n}.$$

Next since g is Lipschitz continuous, so is S_g . Thus, we use Theorem 6 to get

$$|S_g(\sum_{i=1}^d \lambda_i \phi_q(x_i)) - S_g(\sum_{i=1}^d \lambda_i L_q(x_i))| \leq 2C_g \sum_{i=1}^d \lambda_i |\phi_q(x_i) - L_q(x_i)| \leq \frac{d \cdot 2C_g}{(n + 1)}.$$

Let us put the above estimates together to have

$$|f(\mathbf{x}) - \sum_{q=0}^{2d} S_g(\sum_{i=1}^d \lambda_i L_q(x_i))| \leq \frac{(2d + 1)C_g}{2n} + \frac{(2d + 1)2dC_g}{(n + 1)} \leq \frac{(2d + 1)^2 C_g}{n}.$$

The conclusion of Theorem 4 follows. \square

As K-outer function g may not be Lipschitz continuous, we next consider a class of functions which is of Hölder continuity. Letting $\alpha \in (0, 1]$, we say g is in $C^{0, \alpha}$ if

$$\sup_{x, y \in [0, d]} \frac{|g(x) - g(y)|}{|x - y|^\alpha} \leq L_\alpha(g) < \infty. \quad (16)$$

Using such a continuous function g , we can define a multivariate continuous function f by using the formula in Theorem 2. Let us extend the analysis of the proof of Theorem 7 to have

Theorem 8 *Suppose that g is Hölder continuous over $[0, d]$, say $g \in C^{0, \alpha}$ with $L_\alpha(g)$ for some $\alpha \in (0, 1]$. For any $n \geq 1$, there exists a partition Δ with n interior knots such that*

$$\text{dist}(g, S_1^0(\Delta))_\infty \leq \frac{L_\alpha(g)d^\alpha}{2(n + 1)^\alpha}.$$

Similarly, we can define a class of functions which is K-Hölder continuous in the sense that K-outer function g is Hölder continuity $\alpha \in (0, 1)$. For each univariate g in $C^{0, \alpha}([0, d])$, we define f using the KST formula (1). Then we have a new class of continuous functions which will satisfy (17). The proof is a straightforward generalization of the one for Theorem 4, we leave it to the interested readers.

Theorem 9 For each continuous function $f \in C([0, 1]^d)$, let g be the K -outer function associated with f . Suppose that g is in $C^{0,\alpha}([0, d])$ for some $\alpha \in (0, 1]$. Then

$$\inf_{s \in \mathcal{K}_{n,n}(\sigma_1)} \|f - s\|_{C([0,1]^d)} \leq \frac{(2d+1)^2 L_\alpha(g)}{n^\alpha}. \quad (17)$$

Finally, in this section, we study the K -modulus of continuity. For any continuous function $f \in C[0, 1]^d$, let g_f be the K -outer function of f based on the KST. Then we use $\omega(g_f, h)$ which is called the K -modulus of continuity of f to measure the smoothness of g_f . Due to the uniform continuity of g_f , we have linear spline S_{g_f} over an equally-spaced knot sequence such that

$$|g_f(t) - S_{g_f}(t)| \leq \omega(g_f, h), \quad \forall t \in [0, d] \quad (18)$$

for any $h > 0$, e.g. $h = 1/n$ for a positive integer n . It follows that

$$|g_f\left(\sum_{i=1}^d \lambda_i \phi_q(x_i)\right) - S_{g_f}\left(\sum_{i=1}^d \lambda_i \phi_q(x_i)\right)| \leq \omega(g_f, h), \quad (19)$$

for any $(x_1, \dots, x_d) \in [0, 1]^d$. Since $\phi_q, q = 0, \dots, 2d$ are monotonically increasing, we use Theorem 6 to have linear splines L_q such that $|L_q(t) - \phi_q(t)| \leq h$ since $V_0^1(\phi_q) \leq 1$. We now estimate

$$|S_{g_f}\left(\sum_{i=1}^d \lambda_i \phi_q(x_i)\right) - S_{g_f}\left(\sum_{i=1}^d \lambda_i L_q(x_i)\right)| \quad (20)$$

for $q = 0, \dots, 2d$. Note that

$$\left| \sum_{i=1}^d \lambda_i \phi_q(x_i) - \sum_{i=1}^d \lambda_i L_q(x_i) \right| \leq \sum_{i=1}^d |\phi_q(x_i) - L_q(x_i)| \leq dh.$$

The difference of the above two points in $[0, d]$ is separated by at most d subintervals with length h and hence, we will have

$$|S_{g_f}\left(\sum_{i=1}^d \lambda_i \phi_q(x_i)\right) - S_{g_f}\left(\sum_{i=1}^d \lambda_i L_q(x_i)\right)| \leq 2d \cdot \omega(g_f, h) \quad (21)$$

since S_{g_f} is a linear interpolatory spline of g_f . It follows that

$$\begin{aligned} & \left| f(x_1, \dots, x_n) - \sum_{q=0}^{2d} S_{g_f}\left(\sum_{i=1}^d \lambda_i L_q(x_i)\right) \right| \\ & \leq \sum_{q=0}^{2d} |g_f\left(\sum_{i=1}^d \lambda_i \phi_q(x_i)\right) - S_{g_f}\left(\sum_{i=1}^d \lambda_i \phi_q(x_i)\right)| + \sum_{q=0}^{2d} |S_{g_f}\left(\sum_{i=1}^d \lambda_i \phi_q(x_i)\right) - S_{g_f}\left(\sum_{i=1}^d \lambda_i L_q(x_i)\right)| \\ & \leq (2d+1)\omega(g_f, h) + (2d+1)2d \cdot \omega(g_f, h). \end{aligned}$$

Therefore, we conclude the following theorem.

Theorem 10 For any continuous function $f \in C[0, 1]^d$, let g_f be the K -outer function of f in (2). Then

$$\inf_{s \in \mathcal{N}_{(2d+1)dn,n}(\sigma_1)} \|f - s\|_{C([0,1]^d)} \leq (2d+1)^2 \omega(g_f, 1/n), \quad (22)$$

where $\mathcal{N}_{(2d+1)dn,n}(\sigma_1)$ is defined in (5).

3 KB-splines and LKB-splines

However, it is not easy to seek if the K-outer function g_f is Lipschitz continuous when given a continuous functions f . We have to compute g_f from f first. We have implemented Lorentz’s constructive proof of Theorem 2 and plotted the curve g_f for many smooth functions f . Even if f is a linear polynomial in the 2-dimensional space, the K-outer function g still behaviors very badly although we can use K-network with two layers to approximate this linear polynomial f arbitrarily well in theory. We circumvent the difficulty of having such a wildly behaved K-outer function g by introducing KB-splines and LKB-splines in this section. In addition, we will explain how to use them to approximate high dimensional functions.

First of all, we note that the implementation of these $\phi_q, q = 0, \dots, 2d$ is not easy. Numerical ϕ_q ’s are not accurate enough. Indeed, letting $z_q(x_1, \dots, x_d) = \sum_{i=1}^d \lambda_i \phi_q(x_i)$, Consider the transform:

$$T(x_1, \dots, x_d) = (z_0, z_1, \dots, z_{2d}) \tag{23}$$

which maps from $[0, 1]^d$ to \mathbb{R}^{2d+1} . Let $Z = \{T(x_1, \dots, x_d), (x_1, \dots, x_d) \in [0, 1]^d\}$ be the image of $T([0, 1]^d) \subset \mathbb{R}^{2d+1}$. It is easy to see that the image is closed. We know that the map T is one-to-one (cf. [47]) and continuous. As the dimension of Z is much larger than d , the map T is like a well-known Peano curve which maps from $[0, 1]$ to $[0, 1]^2$ and hence, the implementation of T , i.e., the implementation of ϕ_q ’s is not possible to be accurate. However, we are able to compute these ϕ_q and decompose g such that the reconstruction of constant function is exact. Let us present two examples to show that our numerical implementation is reasonable. For convenience, let us use images as 2D functions and compute their K-outer functions g and then reconstruct the images back. In Figures 1–2, we can see that the reconstruction is reasonable although K-outer functions g are oscillating very much. Certainly, these are not continuous functions and hence we do not expect that g to be Lipschitz continuous. But these reconstructed images are a “proof” that our computational code can work.

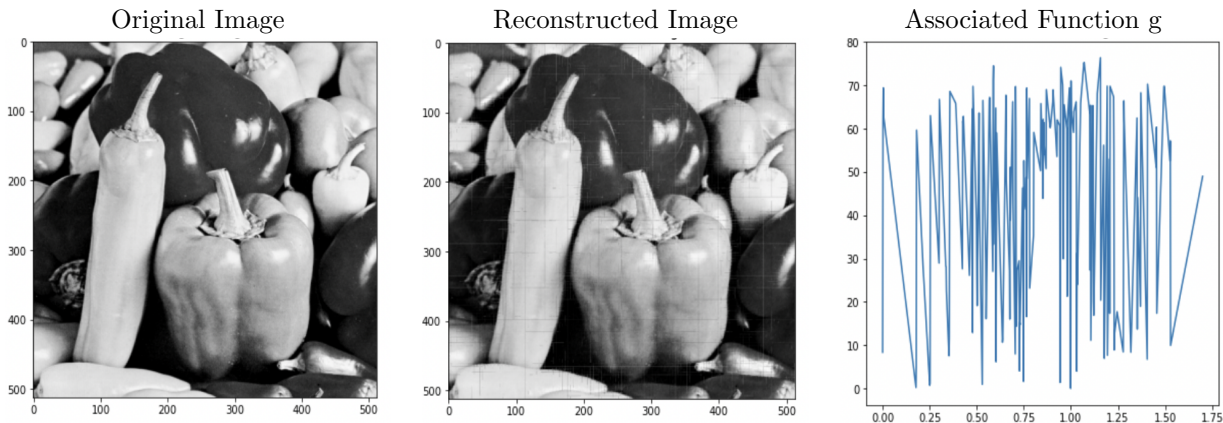


Figure 1: Original image (left) and reconstructed image (middle) based the K-outer function g (right)

Next we present two examples of smooth functions whose K -outer functions may not be Lipschitz continuous in Figure 3. Note that the reconstructed functions are very noisy, in fact they are too noisy to believe that the implementation of the KST can be useful. In order to see that these noisy functions are indeed the original functions, we applied a penalized least squares method based on bivariate spline method (We will explain it below). That is, after denoising, the reconstructed functions are very close to the exact original functions as shown in Figure 3. The denoising method is successful as shown above. This enables us to use this approach to approximate any continuous functions.

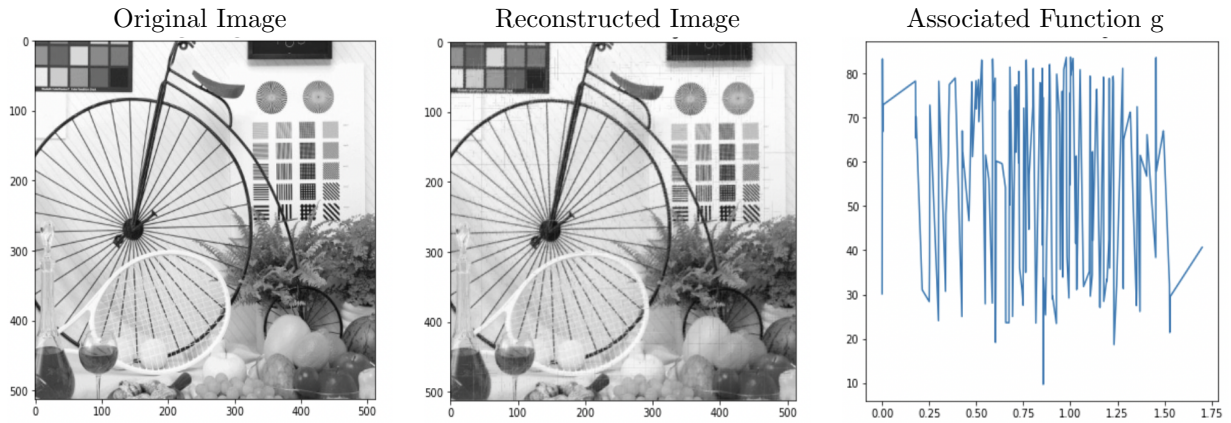


Figure 2: Original image (left) and reconstructed image (middle) based the K-outer function g (right)

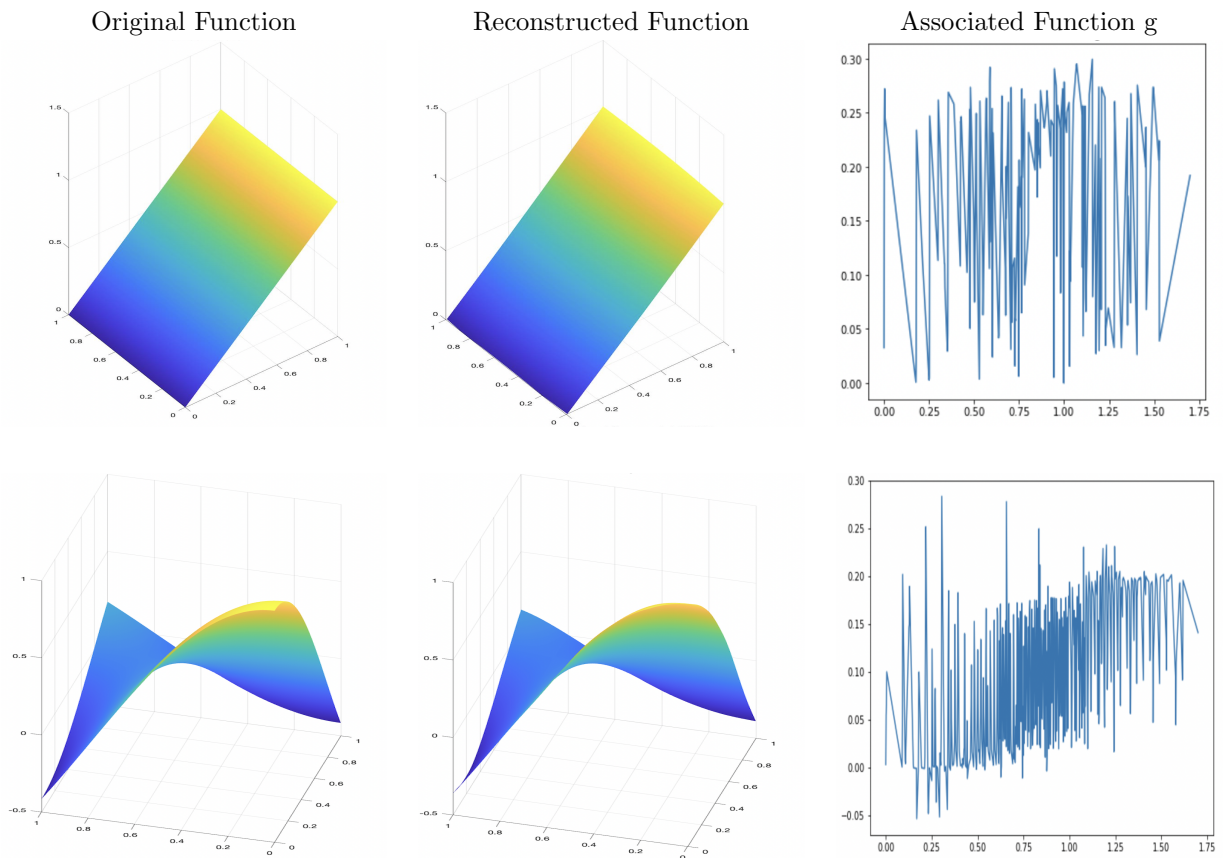


Figure 3: Upper Row: $f(x, y) = x$ (left), reconstructed function (middle), and K-outer function g (right). Lower Row: $f(x, y) = \cos(2x) \cos(2y)$ (left), reconstructed function (middle), and K-outer function g (right).

3.1 KB-splines

To this end, we use standard uniform B-splines to form some subclasses of K-Lipschitz continuous functions. Let $\Delta_n = \{0 = t_1 < t_2 < \dots < t_{dn} < d\}$ be a uniform partition of interval $[0, d]$ and let $b_{n,i}(t) = B_k(t - t_i), i = 1, \dots, dn$ be the standard B-splines of degree k with $k \geq 1$. For simplicity, we only explain our approach based on linear B-splines for the theoretical aspect while using other B-splines (e.g. cubic B-splines) for the numerical experiments. We define KB-splines by

$$KB_{n,j}(x_1, \dots, x_d) = \sum_{q=0}^{2d} b_{n,j} \left(\sum_{i=1}^d \lambda_i \phi_q(x_i) \right), j = 1, \dots, dn. \quad (24)$$

It is easy to see that each of these KB-splines defined above is nonnegative. Due to the property of B-splines: $\sum_{i=1}^{dn} b_{n,i}(t) = 1$ for all $t \in [0, d]$, we have the following property of KB-splines:

Theorem 11 *We have $\sum_{i=1}^{dn} KB_{n,i}(x_1, \dots, x_d) = 1$ and hence, $0 \leq KB_{n,i} \leq 1$.*

Proof. The proof is immediate by using the fact $\sum_{i=1}^{dn} b_{n,i}(t) = 1$ for all $t \in [0, d]$. \square

Remark 1 *We note that a few of these dn KB-splines will be zero since $0 < \lambda_i \leq 1$ and $\min\{\lambda_i, i = 1, \dots, d\} < 1$. The number of zero KB-splines is dependent on the choice of $\lambda_i, i = 1, \dots, d$.*

A more interesting result is

Theorem 12 *The nonzero KB-splines $\{KB_{n,j} \neq 0, j = 1, \dots, dn\}$ are linearly independent.*

Proof. Suppose there are $c_j, j = 1, 2, \dots, dn$ such that $\sum_{j=1}^{dn} c_j KB_{n,j}(x_1, \dots, x_d) = 0$ for all $(x_1, \dots, x_d) \in [0, 1]^d$. Then we want to show $c_j = 0$ for all $j = 1, 2, \dots, dn$. Let us focus on the case $d = 2$ as the proof for general case d is similar. Suppose $n > 0$ is a fixed integer and we use the notation $z_q = \sum_{i=1}^2 \lambda_i \phi_q(x_i)$ as above. Then based on the graphs of ϕ_q in Figure 4, we can choose $x_1 = \delta$ and $x_2 = 0$ with $0 < \delta \leq 1$ small enough such that $KB_{n,j}(x_1, 0) = \sum_{q=0}^4 b_j(z_q(\delta, 0)) = 0$ for all $j = 3, 4, \dots, 2n$. Therefore in order to show the linear independence of $KB_{n,j}, j = 1, 2, \dots, 2n$, it suffices to show $\sum_{j=1}^2 c_j KB_{n,j}(x_1, x_2) = 0$ implies $c_1 = c_2 = 0$. Let us confine $x_1 \in [0, \delta]$ and $x_2 = 0$. Then we have

$$\begin{aligned} 0 &= c_1 KB_{n,1}(x_1, x_2) + c_2 KB_{n,2}(x_1, x_2) = c_1 \left(\sum_{q=0}^4 b_1(z_q) \right) + c_2 \left(\sum_{q=0}^4 b_2(z_q) \right) \\ &= c_1 \left(\sum_{q=0}^4 b_1(z_q) \right) + c_2 \left(5 - \sum_{q=0}^4 b_1(z_q) \right) = (c_1 - c_2) \left(\sum_{q=0}^4 b_1(z_q) \right) + 5c_2, \end{aligned}$$

where we have used the fact that $b_1(x) + b_2(x) = 1$ over $[0, 1/n]$. Since c_2 is constant, and $\sum_{q=0}^4 b_1(z_q)$ is not constant when x_1 varies between 0 and δ , we must have $c_1 = c_2$. Hence $c_2 = 0$ and therefore $c_1 = 0$.

In the same fashion, we can choose \tilde{x}_1 and $\tilde{\delta}$ such that $KB_{n,j} = \sum_{q=0}^4 b_j(z_q(\tilde{x}_1, 0)) = 0$ for all $j = 1, 2, \dots, 2n$ except for $j = k, k + 1$. By the similar argument as above, we have $c_k = c_{k+1} = 0$. By varying k between 1 and $2n$, we get $c_j = 0$ for all $j = 1, 2, \dots, n$. \square

Since $\text{span}\{b_{n,i}, i = 1, \dots, nd\}$ will be dense in $C[0, d]$ when $n \rightarrow \infty$, we can conclude that $\text{span}\{KB_{n,j}, j = 1, \dots, nd\}$ will be dense in $C([0, 1]^d)$. That is, we have

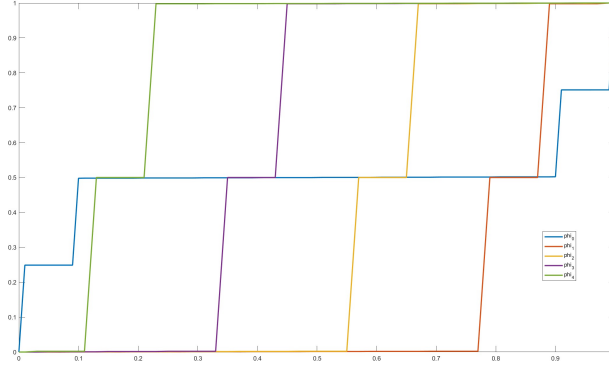


Figure 4: ϕ_q , $q = 0, 1, 2, 3, 4$, in the 2D setting.

Theorem 13 *The KB-splines $KB_{n,j}(x_1, \dots, x_d)$, $j = 1, \dots, nd$, are dense in $C([0, 1]^d)$ when $n \rightarrow \infty$.*

Proof. For any continuous function $f \in C([0, 1]^d)$, let $g_f \in C[0, d]$ be the K-outer function of f . For any $\epsilon > 0$, there is an integer $n > 0$ and a spline $S_{g_f} \in \text{span}\{b_{n,i}, i = 1, \dots, dn\}$ such that

$$\|g_f(t) - S_{g_f}(t)\|_\infty \leq \epsilon/(2d + 1)$$

for all t . Writing $S_{g_f}(t) = \sum_{i=1}^{dn} c_i(f)b_{n,i}(t)$, we have

$$\begin{aligned} & |f(x_1, \dots, x_d) - \sum_{i=1}^{dn} c_i(f)KB_{n,i}(x_1, \dots, x_d)| \\ &= \left| \sum_{q=0}^{2d} g(z_q(x_1, \dots, x_d)) - \sum_{i=1}^{dn} c_i(f) \sum_{q=0}^{2d} b_{n,i}(z_q(x_1, \dots, x_d)) \right| \\ &\leq \sum_{q=0}^{2d} |g(z_q(x_1, \dots, x_d)) - S_{g_f}(z_q(x_1, \dots, x_d))| \leq (2d + 1)\epsilon/(2d + 1) = \epsilon. \end{aligned}$$

This completes the proof. □

3.2 Our LKB-splines

However, in practice, these $KB_{n,j}$'s are very noisy due to any implementation of ϕ_q 's as we have explained before that the functions z_q , $q = 0, \dots, 2d$, like Peano's curve. One has no way to have an accurate implementation. Thus, we have to use a denoising method as shown in a previous subsection. Let us explain a multivariate spline method for denoising for $d = 2$ and $d = 3$. In general, we can use tensor product B-splines for denoising for any $d \geq 2$ which is similar to what we are going to explain below. For convenience, let us consider $d = 2$ and let Δ be a triangulation of $[0, 1]^2$. For any degree $D \geq 1$ and smoothness $r \geq 1$ with $r < D$, let

$$S_D^r(\Delta) = \{s \in C^r([0, 1]^2) : s|_T \in \mathbb{P}_D, T \in \Delta\} \quad (25)$$

be the spline space of degree D and smoothness r with $D > r$. We refer to [39] for a theoretical detail and [2] for a computational detail. For a given data set $\{(x_i, y_i, z_i), i = 1, \dots, N\}$ with $(x_i, y_i) \in [0, 1]^2$

and $z_i = f(x_i, y_i) + \epsilon_i, i = 1, \dots, N$ with noises ϵ_i which may not be very small, the penalized least squares method (cf. [37] and [40]) is to find

$$\min_{s \in S_5^1(\Delta)} \sum_{i=1, \dots, N} |s(x_i, y_i) - z_i|^2 + \lambda \mathcal{E}_2(s) \quad (26)$$

with $\lambda \approx 1$, where $\mathcal{E}_2(s)$ is the thin-plate energy functional defined as follows.

$$\mathcal{E}_2(s) = \int_{\Omega} \left| \frac{\partial^2}{\partial x^2} s \right|^2 + 2 \left| \frac{\partial^2}{\partial x \partial y} s \right|^2 + \left| \frac{\partial^2}{\partial y^2} s \right|^2. \quad (27)$$

Bivariate splines have been studied for several decades and they have been used for data fitting (cf. [37], [40], and [41] and [77]), numerical solution of partial differential equations (see, e.g. [38]), and data denoising (see, e.g. [41]).

We now explain that the penalized least squares method can produce a good smooth approximation of the given data. For convenience, let $S_{f,\epsilon}$ be the minimizer of (26) and write $\|f\|_{\mathcal{P}} = \sqrt{\frac{1}{N} \sum_{i=1}^N |f(x_i, y_i)|^2}$ is the rooted mean squares (RMS). If $f \in C^2([0, 1]^2)$, we have the following

Theorem 14 *Suppose that f is twice differentiable over $[0, 1]^2$. Let $S_{f,\epsilon}$ be the minimizer of (26). Then we have*

$$\|f - S_{f,\epsilon}\|_{\mathcal{P}} \leq C \|f\|_{2,\infty} |\Delta|^2 + 2\|\epsilon\|_{\mathcal{P}} + \sqrt{\lambda \mathcal{E}_2(f)} \quad (28)$$

for a positive constant C independent of f , degree d , and triangulation Δ .

To prove the above result, let us recall the following minimal energy spline $S_f \in S_5^1(\Delta)$ of data function f : letting Δ be a triangulation of $[0, 1]^2$ with vertices $(x_i, y_i), i = 1, \dots, N$, S_f is the solution of the following minimization:

$$\min_{S_f \in S_5^1(\Delta)} \mathcal{E}_2(S_f) : \quad S_f(x_i, y_i) = f(x_i, y_i), (x_i, y_i), i = 1, \dots, N. \quad (29)$$

Then it is known that S_f approximates f very well if $f \in C^2([0, 1]^2)$. We have

Theorem 15 (von Golitschek, Lai and Schumaker, 2002([76])) *Suppose that $f \in C^2([0, 1]^2)$. Then*

$$\|S_f - f\|_{\infty} \leq C \|f\|_{2,\infty} |\Delta|^2 \quad (30)$$

for a positive constant C independent of f and Δ , where $\|f\|_{2,\infty}$ denotes the maximum norm of the second order derivatives of f over $[0, 1]^2$ and $\|S_f - f\|_{\infty}$ is the maximum norm of $S_f - f$ over $[0, 1]^2$.

Proof.[of Theorem 14] Recall that $S_{f,\epsilon}$ is the minimizer of (26). We now use S_f to have

$$\begin{aligned} \|f - S_{f,\epsilon}\|_{\mathcal{P}} &\leq \|z - S_{f,\epsilon}\|_{\mathcal{P}} + \|\epsilon\|_{\mathcal{P}} \leq \sqrt{\|z - S_{f,\epsilon}\|_{\mathcal{P}}^2 + \lambda \mathcal{E}_2(S_{f,\epsilon})} + \|\epsilon\|_{\mathcal{P}} \\ &\leq \sqrt{\|z - S_f\|_{\mathcal{P}}^2 + \lambda \mathcal{E}_2(S_f)} + \|\epsilon\|_{\mathcal{P}} \leq \|f - S_f\|_{\mathcal{P}} + 2\|\epsilon\|_{\mathcal{P}} + \sqrt{\lambda \mathcal{E}_2(f)} \\ &\leq C \|f\|_{2,\infty} |\Delta|^2 + 2\|\epsilon\|_{\mathcal{P}} + \sqrt{\lambda \mathcal{E}_2(f)}, \end{aligned}$$

where we have used a fact that $\mathcal{E}_2(S_f) \leq \mathcal{E}_2(f)$ which can be found in [76]. These complete the theorem of this section. \square

If f is C^2 smooth, then $S_{f,\epsilon}$ will be a good approximation of f when the size $|\Delta|$ of triangulation is small, the thin plate energy $\mathcal{E}_2(f)$ with $\lambda > 0$ is small, and the noises $\|\epsilon\|_{\mathcal{P}}$ is small even though a few individual noises ϵ_i can be large. Note that ϵ can be made small by increasing the accuracy of the implementation of ϕ_q .

Now let us illustrate some examples of the denoised KB-splines in Figure 5. We will call these denoised KB-splines the LKB-splines for simplicity. One can see that the KB-splines are continuous but not smooth functions at all, while the LKB-splines are. With these LKB-splines in hand, we can approximate high dimensional continuous functions accurately. Let us report our numerical results in the next section.

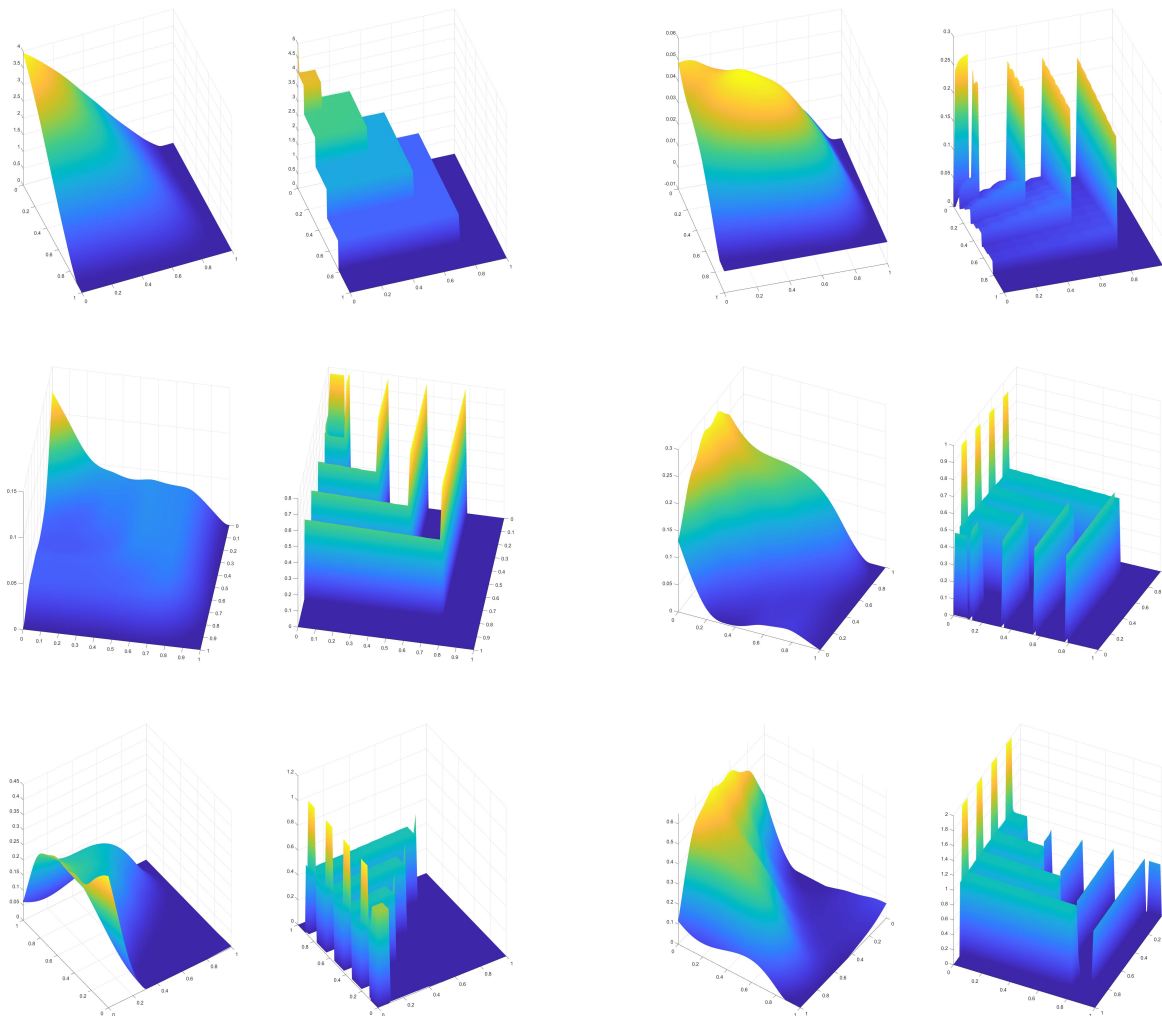


Figure 5: Some Examples of LKB-splines (the first and third columns) which are the smoothed version of the corresponding KB-splines (the second and fourth columns).

4 Numerical Approximation by LKB-splines

4.1 The LKB-splines will be Dense in $C([0, 1]^d)$

First of all, let us see that the LKB-splines can be dense in $C([0, 1]^d)$ when $n \rightarrow \infty$. As we explained above, the KB-splines are dense in $C([0, 1]^d)$. That is, due to the inaccuracy of implementation of ϕ_q , we let $\tilde{\phi}_q$ be the numerical ϕ_q such that $\tilde{\phi}_q(x_i) = \phi_q(x_i) + \epsilon$, where ϵ is not only dependent on q , but also dependent on x_i . Since ϕ_q is a monotone function, we may find \tilde{x}_i such that $\phi_q(x_i) + \epsilon = \phi_q(\tilde{x}_i)$. Thus, it follows that

$$\sum_{i=1}^d \lambda_i \tilde{\phi}_q(x_i) = \sum_{i=1}^d \lambda_i \phi_q(\tilde{x}_i), \quad (31)$$

and hence,

$$\sum_{i=1}^{dn} c_i(f) \sum_{q=0}^{2d} b_{n,i} \left(\sum_{j=1}^d \lambda_j \tilde{\phi}_q(x_j) \right) = \sum_{i=1}^{dn} c_i(f) \sum_{q=0}^{2d} b_{n,i} \left(\sum_{j=1}^d \lambda_j \phi_q(\tilde{x}_i) \right) = f(\tilde{x}_1, \dots, \tilde{x}_d) + O(\epsilon). \quad (32)$$

Due to the linearity of denoising process, writing \mathcal{D} to be the denoising operator, we apply \mathcal{D} to both sides of the equation above and we obtain

$$\sum_{i=1}^{dn} c_i(f) LKB_{n,i}(x_1, \dots, x_d) = \mathcal{D}(f)(x_1, \dots, x_d) + O(\epsilon). \quad (33)$$

When f is a sufficiently smooth, $\mathcal{D}(f)(x_1, \dots, x_d) \approx f(x_1, \dots, x_d)$ or $\mathcal{D}(f)(x_1, \dots, x_d) = f(x_1, \dots, x_d) + O(\eta)$ for $\eta \approx 0$. This gives a heuristic reason that LKB-splines are dense in $C([0, 1]^d)$.

Next let us design numerical experiments to demonstrate that LKB-splines are dense in $C([0, 1]^d)$. We choose 101^d equally-spaced points $\mathbf{x}_i \in [0, 1]^d$ for $d = 2$ and 51^d equally-spaced points over $[0, 1]^d$ for $d = 3$. For any continuous function $f \in C([0, 1]^d)$, we use the function values at these data locations to find an approximation $F_n = \sum_{j=1}^{dn} c_j LKB_{n,j}$ by the discrete least squares method which is the solution of the following minimization

$$\min_{c_j} \left\| f - \sum_{j=1}^{dn} c_j LKB_{n,j} \right\|_{\mathcal{P}}, \quad (34)$$

where $\|f\|_{\mathcal{P}}$ is the RMS semi-norm based on the function values f over these 101^d or 51^d sampled data points in $[0, 1]^d$. We shall report the accuracy $\|f - F_n(f)\|_{\mathcal{P}\mathcal{P}}$, where $\|f\|_{\mathcal{P}\mathcal{P}}$ is the RMS semi-norm based on 401^d function values. The current computational power enables to do the numerical experiments for $d = 2$ with $n = 10, \dots, 10,000$ and for $d = 3$ with $n = 10, \dots, 1000$.

For $d = 2$, we choose the following 10 testing functions across different families of continuous functions to check the computational accuracy.

$$\begin{aligned} f_1 &= x^2; f_2 = xy; f_3 = \sin(x); \\ f_4 &= \tan(x - y) / \tan(1); \\ f_5 &= \sin(\sin(\sin(\sin(x^2 - y^2)))); \\ f_6 &= \exp(1 - (x - 0.5)^2 - (y - 0.5)^2) / \exp(1); \\ f_7 &= \log(1 + x^2 + y^2) / \log(4); \\ f_8 &= (x + 2y) / (3(1 + y^2 + x^2)); \\ f_9 &= \tan(x^2 - y^2) / \tan(1); \\ f_{10} &= \exp(-\cos(1 + \sin(1 + \cos(x^2 - y^2)))) / \exp(1); \end{aligned}$$

Table 1: RMSEs of the Discrete Least Squares Fitting (34) of 10 Testing Functions Using n Number of LKB-splines in 2D.

| Testing Funs | $n = 10$ | $n = 100$ | $n = 1000$ | $n = 10000$ |
|--------------|-----------|-----------|------------|-------------|
| f_1 | 1.126e-02 | 2.610e-04 | 1.200e-04 | 1.248e-07 |
| f_2 | 2.865e-03 | 7.269e-04 | 2.590e-05 | 1.577e-08 |
| f_3 | 3.609e-03 | 7.526e-05 | 3.407e-05 | 4.203e-08 |
| f_4 | 2.969e-03 | 2.974e-04 | 1.453e-04 | 2.460e-07 |
| f_5 | 1.886e-02 | 7.694e-04 | 3.071e-04 | 2.106e-07 |
| f_6 | 4.513e-03 | 1.828e-04 | 6.697e-05 | 6.484e-08 |
| f_7 | 1.957e-03 | 8.415e-05 | 4.009e-05 | 6.345e-08 |
| f_8 | 2.685e-03 | 1.065e-04 | 3.946e-05 | 2.434e-08 |
| f_9 | 2.058e-02 | 1.333e-03 | 6.295e-04 | 1.096e-06 |
| f_{10} | 1.502e-03 | 8.060e-05 | 3.472e-05 | 5.492e-08 |

For $d = 3$, we choose the following 10 testing functions across different families of continuous functions to check the computational accuracy.

$$\begin{aligned}
 f_1 &= xyz; f_2 = x^2y; f_3 = \sin(x^2 + y^2 + z^2); \\
 f_4 &= \log(4 + x^3 - y^2 + z)/\log(6); f_5 = (x + z + y)/(3(1 + y^2 + x^2 + z^2)); \\
 f_6 &= \cos(1/(1 + xyz)); f_7 = \sin(2\pi(x + y + z)); \\
 f_8 &= \sin(1 + \sin(x + \sin(y + \sin(z)))); f_9 = \exp(1 - (x^2 + y^2 + z^2)/2)/\exp(1); \\
 f_{10} &= (1 + x^2 + y^3 + z^4)/(4(1 + x^2 + y^2 + z^2));
 \end{aligned}$$

The computational results are reported in Table 1 and Table 2. We can see that the RMSEs are small as n gets large and hence these LKB splines are dense in $C([0, 1]^d)$ for $d = 2$ and $d = 3$. We also see that these computational results are compatible with the order of convergence given in Theorem 4.

Table 2: RMSEs of the Discrete Least Squares Fitting (34) of 10 Testing Functions Using n Number of LKB-splines in 3D.

| Testing Funs | $n = 10$ | $n = 100$ | $n = 1000$ |
|--------------|-----------|-----------|------------|
| f_1 | 7.826e-03 | 6.051e-05 | 3.123e-05 |
| f_2 | 2.743e-03 | 1.060e-04 | 3.733e-05 |
| f_3 | 3.164e-02 | 3.494e-04 | 1.495e-04 |
| f_4 | 1.003e-02 | 4.088e-05 | 1.074e-05 |
| f_5 | 9.337e-03 | 9.886e-05 | 2.873e-05 |
| f_6 | 6.896e-03 | 1.029e-04 | 2.674e-05 |
| f_7 | 6.596e-01 | 1.180e-02 | 1.022e-02 |
| f_8 | 9.020e-03 | 5.161e-05 | 3.336e-05 |
| f_9 | 7.096e-03 | 6.260e-05 | 1.839e-05 |
| f_{10} | 4.250e-03 | 6.323e-05 | 2.179e-05 |

4.2 The Magic Data Locations for Breaking the Curse of Dimension

For convenience, let us use X_{data} to indicate the data matrix of the discrete least squares problem (34). In other words, for $1 \leq j \leq dn$, the j th column $X_{data}(:, j)$ consists of $\{LK B_{n,j}(\mathbf{x}_i)\}$ where $\mathbf{x}_i \in [0, 1]^2$

are those 101^2 equally-spaced sampled points in 2D or $\mathbf{x}_i \in [0, 1]^3$ are those 51^3 equally-spaces sampled points in 3D. Clearly, the experiment above requires 101^d or 51^d data values which suffers from the curse of dimension. However, we in fact do not need such many data values. Our main reason is that the observation matrix X_{data} has many zero columns or near zero columns due to the fact many locations from 101^2 or 51^3 equally-spaced points do not fall into the support of linear B-splines based on the map z_q . The structures of X_{data} are shown for the case of $n = 100$ and $n = 1000$ when $d = 2$.



Figure 6: The spy of the observation matrices for $n = 100$ and $n = 1000$ when $d = 2$.

That is, there are many columns in X_{data} whose entries are zero or near zero. Therefore, there exists a sparse solution to the discrete least squares fitting problem. We adopt the well-known orthogonal matching pursuit (OMP) (cf. e.g. [42]) to find the solution. For convenience, let us explain the sparse solution technique as follows. Over 101^d points $\mathbf{x}_i \in [0, 1]^d$, the columns in the matrix

$$X_{data} = [LKB_{n,j}(\mathbf{x}_i)]_{i=1,\dots,101^d,j=1,\dots,dn} \quad (35)$$

are not linearly independent. Let Φ be the normalized matrix of X_{data} in (35) and $\mathbf{b} = [f(\mathbf{x}_i)]_{i=1,\dots,101^d}$. Write $\mathbf{c} = (c_1, \dots, c_{dn})^\top$, we look for

$$\min \|\mathbf{c}\|_0 : \Phi \mathbf{c} = \mathbf{b} \quad (36)$$

where $\|\mathbf{c}\|_0$ stands for the number of nonzero entries of \mathbf{c} . See many numerical methods in ([42]).

The near zero columns in Φ also tell us that the observation matrix associated with (34) of size $101^d \times dn$ is not full rank $r < dn$. The LKB-splines associated with these columns do not play a role. Therefore, we do not need all dn LKB-splines. This fact is also the reason that one does not need all 101^d data locations and function values due to the linear independence of the associated KB splines. Indeed, let us continue to explain that many data locations from 101^d or 51^d do not play an essential role.

To this end, we use the so-called matrix cross approximation (see [23], [25], [51], [20], [26], [1] and the literature therein). Write $M = X_{data}$ for simplicity and let $r \geq 1$ be a rank of the approximation. It is known (cf. [23]) that when $M_{I,J}$ of size $r \times r$ has the maximal volume among all submatrices of M of size $r \times r$,

$$\|X_{data} - M_{:,J}M_{I,J}^{-1}M_{I,:}\|_C \leq (1+r)\sigma_{r+1}(X_{data}), \quad (37)$$

where $\|\cdot\|_C$ is the Chebyshev norm of matrix and $\sigma_{r+1}(X_{data})$ is the $r+1$ singular value of X_{data} , $M_{I,:}$ is the row block of M associated with the indices in I and $M_{:,J}$ is the column block of M associated with the indices in J . The volume of a square matrix A is the absolute value of the determinant of A .

One mainly needs to find a submatrix $M_{I,J}$ of M such that $M_{I,J}$ has the maximal volume among all $r \times r$ submatrices of M . In practice, we use the concept called dominant matrix to replace the

maximal volume. There are several algorithms, e.g. maxvol algorithm, available in the literature. One of the authors has developed a few greedy based maximal volume search algorithms with Kenneth Allen (cf. [1]). These greedy based maxvol algorithms enable us to find a good submatrix $M_{I,J}$ and solve a much simpler discrete least squares problem $M_{I,J}\hat{\mathbf{x}} \approx \mathbf{f}_I$ where $\mathbf{f} = [\mathbf{f}_I; \mathbf{f}_{I^c}]$ consists of two parts according to the indices in I and the complement indices in I^c . According to Theorem 5.1 in [1], that $\hat{\mathbf{x}}$ is a good approximation of \mathbf{x}_f , the least squares solution vector (34) for a continuous function $f \in C([0, 1]^d)$. More precisely, we have

Theorem 16 (Allen and Lai, 2022 [1]) *For simplicity, let $A = X_{data}$. Let the residual vector $A\mathbf{x}_f - \mathbf{f} = \epsilon$ and $\epsilon = [\epsilon_I; \epsilon_{I^c}]$. Then we have*

$$\|A\hat{\mathbf{x}} - \mathbf{b}\|_\infty \leq \|\epsilon_I\|_1 + \frac{(r+1)}{\sqrt{1 + \frac{r\sigma_{r+1}^2(A)}{(r+1)\|A\|_2^2}}} \sigma_{r+1}(A) \|\mathbf{x}_f\|_1 + \|\epsilon_{I^c}\|_\infty. \quad (38)$$

Let us call the data locations associated with the row indices I magic data locations. We now present some numerical results to demonstrate that the numerical approximation based on the magic data locations is similar to the 101×101 data set in 2D and $51 \times 51 \times 51$ in 3D.

Example 1 *We use 100 testing functions (attached in appendix) in 2D and compute the RMSEs of approximation by using $n = 100$ and $n = 1000$ LKB-splines to show the performance of the two discrete least squares problems: the top one in Figure 7 is the computational results based on $n = 100$. We used 101×101 equally-spaced points over $[0, 1]^2$ as the data locations and the function values over these points to compute the least squares solution for 100 testing functions; The RMSEs are shown in red on the top-right and the RMSEs of the approximation based on the magic set of locations are shown in blue. In the bottom of Figure 7, we show the computational results using $n = 1000$ LKB splines. We can see that the RMSEs based on the magic sets are about 2–3 times than the RMSEs based on 101×101 data locations and values. For reproductivity of Figure 7, a demo program for reproducing this example can be found at <https://github.com/zzzzms/KST4FunApproximation>.*

Example 2 *We also use 100 testing functions (attached in appendix) in 3D and compute the RMSEs of the approximation to show the performance of the two discrete least squares problems: first one is based on $51 \times 51 \times 51$ equally-spaced points over $[0, 1]^3$ as the data locations and the function values over these points to have the least squares solution; second one is based on the magic set of locations when using $n = 100$ and $n = 1000$ LKB splines. In the top of Figure 8, the computational results using $n = 100$ LKB splines are shown and the bottom of Figure 8 is the computational results using $n = 1000$ LKB splines. We can see that the RMSEs based on the magic set are about 2–3 times than the RMSEs based on $51 \times 51 \times 51$ data locations and values.*

Remark 2 *We remark that a magic data set depends on the initial sampled data, and the size of magic data will be larger if the initial sampled data is larger. For example, if instead of using 101×101 equally-spaced points over $[0, 1]^2$, we use 201×201 equally-spaced points, then the location of the magic data points are different and the size of magic data set is bigger than the ones shown in Figure 7.*

Remark 3 *Also, we remark that we can use randomized data locations instead of equally-spaced points over $[0, 1]^d$. Then the location of the magic data points are also different and it will possibly result in a better approximation. We leave the discussion in [63].*

Remark 4 *Finally, our numerical experiments show that there are many functions such as $f(x, y) = \sin(10\pi x) \sin(10\pi y)$ or $f(x, y) = \tanh(\frac{1}{\alpha}((2x-1)^2 + (2y-1)^2 - 0.25)) - \tanh(3/4\alpha)$ for $\alpha = 0.01$, and*

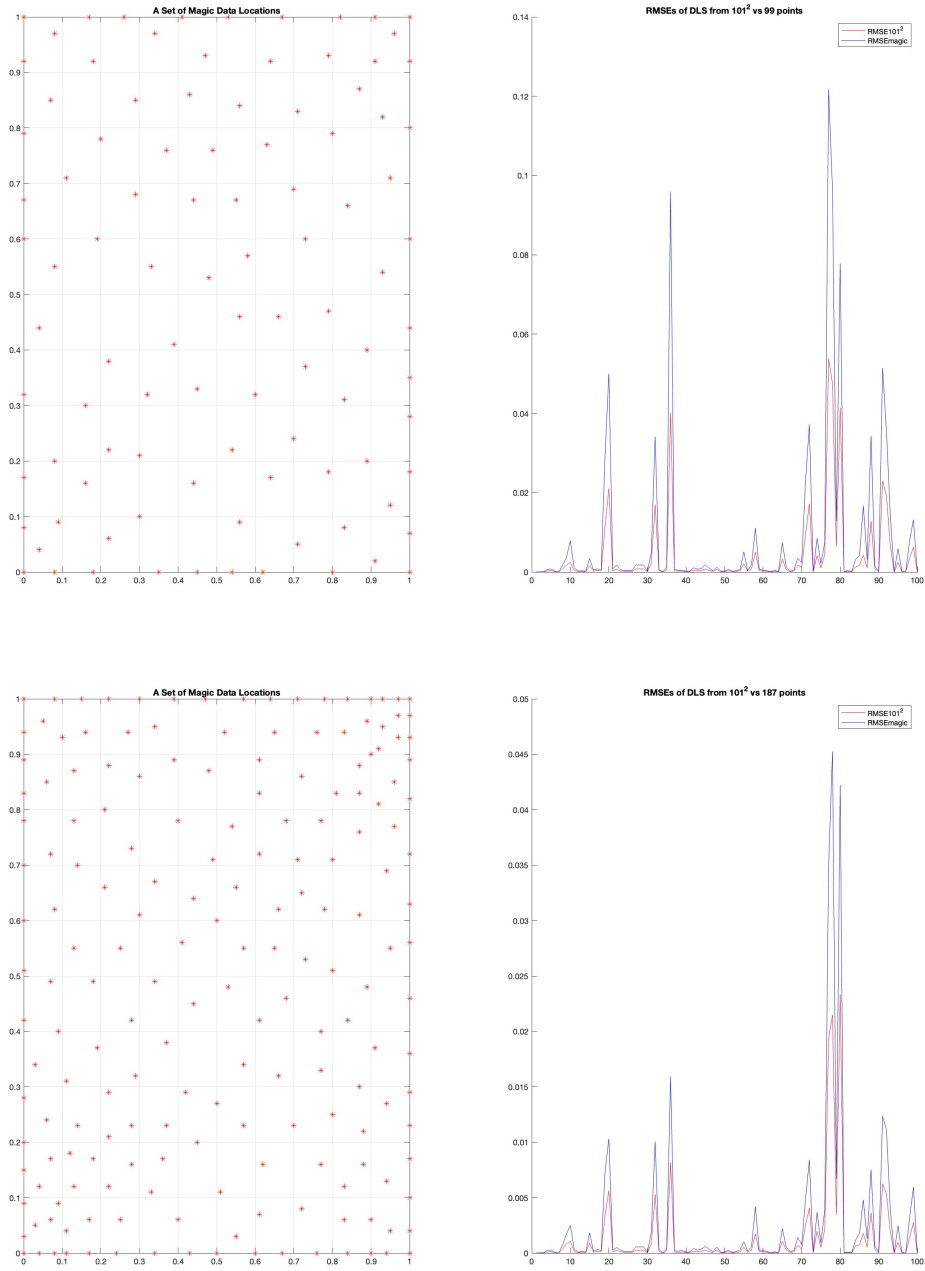


Figure 7: The Magic Data Set of 99 and 187 Locations (left column) and RMSEs of 100 Testing Functions in 2D (right column) (Top Row: $n = 100$. Bottom Row: $n = 1000$).

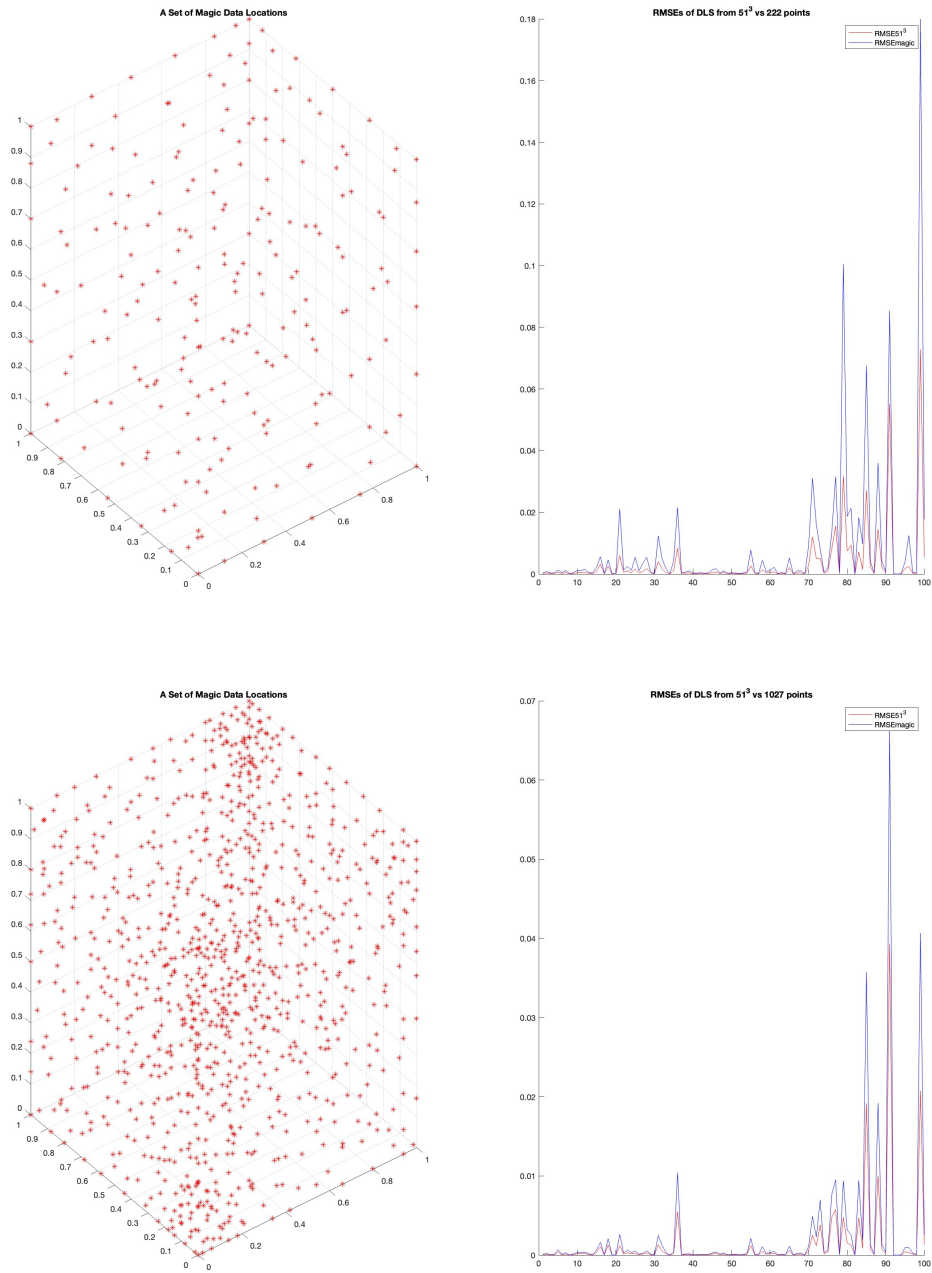


Figure 8: The Magic Data Set of 222 and 1027 Locations (left column) and RMSEs of 100 Testing Functions in 3D (right column) (Top Row: $n = 100$. Bottom Row: $n = 1000$).

their 3D counterparts that our LKB-splines can not well approximate them based on the magic data sets above. Such highly oscillated functions are hard to approximate even using other methods such as multivariate splines. One indeed needs a lot of the data (points and the function values over the points) to approximate them well. It is the same for using the LKB-splines.

We therefore conclude that the curse of dimensionality for the 2D and 3D function approximation can be broken if we use LKB-splines and some magic data sets when f is not very oscillated.

References

- [1] K. Allen and M.-J. Lai, On Matrix Cross Approximation and Its Application, submitted for publication, 2022.
- [2] G. Awanou, M. -J. Lai, P. Wenston, The multivariate spline method for scattered data fitting and numerical solutions of partial differential equations, *Wavelets and splines: Athens (2005)*, 24–74.
- [3] F. Bach, Breaking the curse of dimensionality with convex neural networks, *Journal of Machine Learning Research*, vol. 18, 2017, 1–53.
- [4] A. R. Barron. Universal approximation bounds for superpositions of a sigmoidal function, *IEEE Transactions on Information theory*, 39(3):930–945, 1993.
- [5] B J. Braun, An Application of Kolmogorov’s Superposition Theorem to Function Reconstruction in Higher Dimensions, PhD thesis, University of Bonn, 2009.
- [6] B. J. Braun and M. Griebel, On a constructive proof of Kolmogorov’s superposition theorem, *Constructive Approximation*, 30(3):653–675, 2009.
- [7] D. W. Bryant. Analysis of Kolmogorov’s superposition theorem and its implementation in applications with low and high dimensional data. PhD thesis, University of Central Florida, 2008
- [8] K. Chen, The upper bound on knots in neural networks, arXiv:1611.09448v2 [stat.ML] 30 Nov 2016.
- [9] G. Cybenko, Approximation by Superpositions of a Sigmoidal Function, *Math. Control Signals Systems (1989)* 2:303–314.
- [10] I. Daubechies, R. DeVore, S. Foucart, B. Hanin, and G. Petrova, Nonlinear Approximation and (Deep) ReLU Networks, arXiv:1905.02199v1 [cs.LG] 5 May 2019.
- [11] R. DeVore, R. Howard, and C. Micchelli, Optimal nonlinear approximation, *Manuscripta Mathematica*, 63(4):469–478, 1989.
- [12] R. DeVore, B. Hanin, and G. Petrova, Neural Network Approximation, *Acta Numerica*, 2021, pp. xxx–xxx.
- [13] R. Doss, On the representation of continuous functions of two variables by means of addition and continuous functions of one variable. *Colloquium Mathematicum*, X(2):249–259, 1963.
- [14] Weinan E, Machine Learning and Computational Mathematics, arXiv:2009.14596v1 [math.NA] 23 Sept. 2020.

- [15] Weinan E, Chao Ma and Lei Wu, Barron spaces and the flow-induced function spaces for neural network models, arXiv:1906.08039, 2019.
- [16] Weinan E and Stephan Wojtowytsch, Representation formulas and pointwise properties for Barron functions, arXiv:2006.05982, 2020.
- [17] Weinan E and Stephan Wojtowytsch, On the Banach spaces associated with multilayer ReLU networks: Function representation, approximation theory and gradient descent dynamics, <https://arxiv.org/pdf/2007.15623.pdf>, 2020.
- [18] B. L. Friedman, An improvement in the smoothness of the functions in Kolmogorov’s theorem on superpositions. *Doklady Akademii Nauk SSSR*, 117:1019–1022, 1967.
- [19] Z. Feng, Hilbert’s 13th problem. PhD thesis, University of Pittsburgh, 2010.
- [20] Irina Georgieva and Clemens Hofreither, On the Best Uniform Approximation by Low-Rank Matrices, *Linear Algebra and its Applications*, vol.518(2017), Pages 159–176.
- [21] Girosi, F., & Poggio, T. (1989). Representation properties of networks: Kolmogorov’s theorem is irrelevant. *Neural Computation*, 1(4), 465-469.
- [22] I. Goodfellow, Y. Bengio, A. Courville, *Deep Learning*, MIT Press, 2016.
- [23] S. A. Goreinov and E. E. Tyrtyshnikov, The maximal-volume concept in approximation by low-rank matrices, *Contemporary Mathematics*, 208: 47–51, 2001.
- [24] S. A. Goreinov, E. E. Tyrtyshnikov, and N. L. Zamarashkin, A Theory of Pseudoskeleton Approximations, *Linear Algebra and Its Applications*, 261: 1–21 (1997).
- [25] S. A. Goreinov, I. V. Oseledets, D. V. Savostyanov, E. E. Tyrtyshnikov, N. L. Zamarashkin, How to find a good submatrix, in: *Matrix Methods: Theory, Algorithms, Applications*, (World Scientific, Hackensack, NY, 2010), pp. 247–256.
- [26] N. Kishore Kumar and J. Schneider, Literature survey on low rank approximation of matrices, *Journal on Linear and Multilinear Algebra*, vol. 65 (2017), 2212–2244.
- [27] M. Hansson and C. Olsson, Feedforward neural networks with ReLU activation functions are linear splines, Bachelor Thesis, Univ. Lund, 2017.
- [28] R. Hecht-Nielsen. Kolmogorov’s mapping neural network existence theorem. In *Proceedings of the international conference on Neural Networks*, volume 3, pages 11–14. New York: IEEE Press, 1987.
- [29] K. Hornik. Approximation capabilities of multilayer feedforward networks. *Neural networks* 4, no. 2 (1991): 251-257.
- [30] B. Igel'nik and N. Parikh. Kolmogorov’s spline network. *IEEE Transactions on Neural Networks*, 14(4):725–733, 2003.
- [31] J.-P. Kahane. Sur le Théorème de Superposition de Kolmogorov. *Journal of Approximation Theory*, 13:229–234, 1975.
- [32] H. Katsuura and D. Sprecher. Computational aspects of Kolmogorov’s superposition theorem. *Neural Networks*, 7(3):455–461, 1994.

- [33] J. M. Klusowski and Barron, A.R.: Approximation by combinations of relu and squared relu ridge functions with ℓ_1 and ℓ_0 controls. *IEEE Transactions on Information Theory* 64(12), 7649–7656 (2018).
- [34] A. N. Kolmogorov. The representation of continuous functions of several variables by superpositions of continuous functions of a smaller number of variables. *Doklady Akademii Nauk SSSR*, 108(2):179–182, 1956.
- [35] A. N. Kolmogorov, On the representation of continuous function of several variables by superposition of continuous function of one variable and its addition, *Dokl. Akad. Nauk SSSR* 114 (1957), 369–373.
- [36] V. Kurkov, Kolmogorov’s Theorem and Multilayer Neural Networks, *Neural Networks*, Vol. 5, pp. 501– 506, 1992.
- [37] M. -J. Lai, *Multivariate splines for Data Fitting and Approximation*, the conference proceedings of the 12th Approximation Theory, San Antonio, Nashboro Press, (2008) edited by M. Neamtu and Schumaker, L. L. pp. 210–228.
- [38] M.-J. Lai and J. Lee, A multivariate spline based collocation method for numerical solution of partial differential equations, *SIAM J. Numerical Analysis*, vol. 60 (2022) pp. 2405–2434.
- [39] M. -J. Lai and L. L. Schumaker, *Spline Functions over Triangulations*, Cambridge University Press, 2007.
- [40] M. -J. Lai and L. L. Schumaker, Domain Decomposition Method for Scattered Data Fitting, *SIAM Journal on Numerical Analysis*, vol. 47 (2009) pp. 911–928.
- [41] M. -J. Lai and Wang, L., Bivariate penalized splines for regression, *Statistica Sinica*, vol. 23 (2013) pp. 1399–1417.
- [42] M. -J. Lai and Y. Wang, *Sparse Solutions of Underdetermined Linear Systems and Their Applications*, SIAM Publication, 2021.
- [43] M. Laczkovich, A superposition theorem of Kolmogorov type for bounded continuous functions, *J. Approx. Theory*, vol. 269(2021), 105609.
- [44] X. Liu, *Kolmogorov Superposition Theorem and Its Applications*, Ph.D. thesis, Imperial College of London, UK, 2015.
- [45] J. Lu, Z. Shen, H. Yang, S. Zhang, Deep Network Approximation for Smooth Functions, *SIAM Journal on Mathematical Analysis*, 2021.
- [46] G. G. Lorentz, Metric entropy, widths, and superpositions of functions, *Amer. Math. Monthly*, 69 (1962), 469–485.
- [47] G. G. Lorentz, *Approximation of Functions*, Holt, Rinehart and Winston, Inc. 1966.
- [48] V. E. Maiorov, On best approximation by ridge functions, *J. Approx. Theory* 99 (1999),68–94.
- [49] S. Mallat, Understanding Deep Convolutional Network, *Philosophical Transactions A*, in 2016.
- [50] H. Mhaskar, C. A. Micchelli, Approximation by superposition of sigmoidal and radial basis functions, *Adv. Appl. Math.* 13 (3) (1992) 350–373.

- [51] A. Mikhaleva and I. V. Oseledets, Rectangular maximum-volume submatrices and their applications, *Linear Algebra and its Applications*, Vol. 538, 2018, Pages 187–211.
- [52] Ivan Oseledets and Eugene Tyrtyshnikov, TT-cross approximation for multidimensional arrays, *Linear Algebra and its Applications*, 432 (2010) 70–88.
- [53] H. Montanelli and H. Yang, Error Bounds for Deep ReLU Networks using the Kolmogorov–Arnold Superposition Theorem. *Neural Networks*, 2020.
- [54] H. Montanelli, H. Yang, Q. Du, Deep ReLU Networks Overcome the Curse of Dimensionality for Bandlimited Functions. *Journal of Computational Mathematics*, 2021.
- [55] S. Morris, Hilbert 13: are there any genuine continuous multivariate real-valued functions? *Bulletin of AMS*, vol. 58. No. 1 (2021), pp 107–118.
- [56] M. Nees, Approximative versions of Kolmogorov’s superposition theorem, proved constructively, *J. Comp. Applied Math*, 54(1994), 239–250.
- [57] A. Pinkus, Approximation theory of the MLP model in neural networks, *Acta Numerica* (1999), pp. 143–195.
- [58] P. P. Petrushev, Approximation by ridge functions and neural networks, *SIAM J. Math. Anal.* 30 (1998), 155–189.
- [59] M. J. Powell, *Approximation theory and methods*, Cambridge University Press, 1981.
- [60] J. Schmidt-Hieber, The Kolmogorov-Arnold representation theorem revisited. *Neural Networks*, 137 (2021), 119-126.
- [61] L. L. Schumaker, *Spline Functions: Basic Theory*, Third Edition, Cambridge University Press, 2007.
- [62] J. W. Segel and J. Xu, Approximation rates for neural networks with general activation functions, arXiv:1904.02311v5, May, 2020.
- [63] Zhaiming Shen, *Sparse Solutions for Graph Clustering and High Dimensional Function Approximation*. Ph.D. Dissertation, University of Georgia, 2023.
- [64] Z. Shen, H. Yang, S. Zhang. *Neural Network Approximation: Three Hidden Layers Are Enough*. *Neural Networks*, 2021
- [65] J. W. Siegel and J. Xu. High-Order Approximation Rates for Neural Networks with $(ReLU)^k$ Activation Functions, arXiv:2012.07205 (2020).
- [66] Sho Sonoda and Noboru Murata, Neural network with unbounded activation functions is universal approximator, arXiv:1505.03654v2 [cs.NE] 29, Nov 2015. *J. Applied Comput. Harmonic Analysis*, 43 (2017) 233–268.
- [67] D. A. Sprecher, Ph.D. Dissertation, University of Maryland, 1963.
- [68] D. A. Sprecher, A representation theorem for continuous functions of several variables, *Proc. Amer. Math. Soc.* 16 (1965), 200–203.
- [69] D. A. Sprecher, On the structure of continuous functions of several variables. *Transactions of the American Mathematical Society*, 115:340–355, 1965.

- [70] D. A. Sprecher, On the structure of representation of continuous functions of several variables as finite sums of continuous functions of one variable. *Proceedings of the American Mathematical Society*, 17(1):98–105, 1966.
- [71] D. A. Sprecher, An improvement in the superposition theorem of Kolmogorov. *Journal of Mathematical Analysis and Applications*, 38(1):208–213, 1972.
- [72] D. A. Sprecher, A universal mapping for Kolmogorov’s superposition theorem. *Neural Networks*, 6(8):1089–1094, 1993.
- [73] D. A. Sprecher, A numerical implementation of Kolmogorov’s superpositions. *Neural Networks*, 9(5):765–772, 1996.
- [74] D. A. Sprecher, A Numerical Implementation of Kolmogorov’s Superpositions II. *Neural Networks*, 10(3):447–457, 1997.
- [75] D. A. Sprecher and S. Draghici, Space-filling curves and Kolmogorov superposition based neural networks. *Neural networks: the official journal of the International Neural Network Society*, 15(1):57–67, 2002.
- [76] M. Von Golitschek, Lai, M. -J. and Schumaker, L. L., Bounds for Minimal Energy Bivariate Polynomial Splines, *Numerisch Mathematik*, vol. 93 (2002) pp. 315–331.
- [77] L. Wang, G. Wang, M. -J. Lai, and Gao, L., Efficient Estimation of Partially Linear Models for Spatial Data over Complex Domains, *Statistica Sinica*, vol. 30 (2020) pp. 347–360.
- [78] S. Wojtowytsch and W. E. Can shallow neural networks beat the curse of dimensionality? A mean field training perspective. *IEEE Transactions on Artificial Intelligence*, 1(2):121–129, Oct 2020.
- [79] D. Yarotsky, Error bounds for approximations with deep ReLU networks, *Neural Netw.* 94 (2017) 103-114.
- [80] D. Yarotsky and A. Zhevnerchuk, The phase diagram of approximation rates for deep neural networks, arXiv:1906.09477v2 [cs.NE] 5 Jan 2021.

5 Supplementary Materials

We have used the following 100 testing functions in 2D and 3D for testing the LKB spline approximation. Numerical results are presented in Examples 1 and 2. For convenience, let us include them.

5.1 100 Testing Functions in 2D

```
function ff=testfunctions_2d(x,y,caseNum)

switch caseNum
    case 1
        ff = @(x,y) 1-x+x;
    case 2
        ff = @(x,y) x;
    case 3
        ff = @(x,y) y;
```

```

case 4
    ff = @(x,y) x.^2;
case 5
    ff = @(x,y) y.^2;
case 6
    ff = @(x,y) x.*y;
case 7
    ff = @(x,y) (x+y)/2;
case 8
    ff = @(x,y) x.^3+y.^4;
case 9
    ff = @(x,y) x.^5+y.^6;
case 10
    ff = @(x,y) (x-y).^9;
case 11
    ff = @(x,y) x.^3./(1+y.^2);
case 12
    ff = @(x,y) (1+3*x+4*y)./(1+x.*y);
case 13
    ff = @(x,y) (1+x.^2+y.^2)./(5-x-y.^2);
case 14
    ff = @(x,y) 1./(1+x.^2+y.^2);
case 15
    ff = @(x,y) (x.^10+y.^5)/2;
case 16
    ff = @(x,y) ((1+2*x+4*y)/7).^3;
case 17
    ff = @(x,y) ((1+2*x+ 3*y)/6).^9;
case 18
    ff = @(x,y) ((1+2*x+ 3*y)/6).^5;
case 19
    ff = @(x,y) sin(5*x+6*y);
case 20
    ff = @(x,y) sin(2*pi*(x.^2+y.^2));
case 21
    ff = @(x,y) tan(x-y/2);
case 22
    ff = @(x,y) sin(x.^2-y.^2);
case 23
    ff = @(x,y) cos(x.^2-y.^2);
case 24
    ff = @(x,y) sin(1+cos(x.^2-y.^2));
case 25
    ff = @(x,y) cos(1+sin(1+cos(x.^2-y.^2)));
case 26
    ff = @(x,y) exp(-cos(1+sin(1+cos(x.^2-y.^2))));
case 27
    ff = @(x,y) sin(sin(sin(sin(x.^2-y.^2))));
case 28
    ff = @(x,y) sin(sin(sin(sin(sin(x.^2-y.^2))));
case 29
    ff = @(x,y) sin(sin(sin(sin(sin(sin(x.^2-y.^2))))));
case 30
    ff = @(x,y) 1./(3+sin(sin(sin(sin(x.^2-y.^2))));

```

```

case 31
    ff = @(x,y) cos(5*x).*cos(4*y);
case 32
    ff = @(x,y) sin(5*x).^2;
case 33
    ff = @(x,y) tan(x).*tan(y);
case 34
    ff = @(x,y) tan(x/2).*tan(y/2);
case 35
    ff = @(x,y) (x-2*y).*sin(2*x-y);
case 36
    ff = @(x,y) sin(10*x).*sin(10*y);
case 37
    ff = @(x,y) (x.^2-y.^2)./(1+sin(x).^2+sin(y).^2);
case 38
    ff = @(x,y) cos(x.^2-y.^2)./(1+x.^2+y.^3);
case 39
    ff = @(x,y) sin(1+cos(x.^2-y.^2))./(1+cos(pi*x/2));
case 40
    ff = @(x,y) sin(1+log(1+x.^2+y.^2));
case 41
    ff = @(x,y) log(1+x.^2+y.^2)/log(3);
case 42
    ff = @(x,y) x.*exp(1-x.^2-y.^2);
case 43
    ff = @(x,y) y.*log(1+x.^2+y.^2);
case 44
    ff = @(x,y) x.^2.*log(1+x.^2+y.^2);
case 45
    ff = @(x,y) y.^2.*exp(1-x.^2-y.^2);
case 46
    ff = @(x,y) x.*y.*log(1+x.^2+y.^2).*sin(pi*x+y);
case 47
    ff = @(x,y) sin(x+y).*log(1+x.^2+y.^2);
case 48
    ff = @(x,y) log(x.^2-y.^3+2)/log(3);
case 49
    ff = @(x,y) (log(5+ x.^3))./log(3+y.^2);
case 50
    ff = @(x,y) log(1+x.^2+y.^2)./(1+x.^2+y.^2);
case 51
    ff = @(x,y) (x+ y.^2).^2./(3+sin(x+y.^2));
case 52
    ff = @(x,y) sin(x).^3./(3+sin(y).^2);
case 53
    ff = @(x,y) sin(x+y)./(1+x.^2+y.^2);
case 54
    ff = @(x,y) cos(x.^2+1./(1+x.*y));
case 55
    ff = @(x,y) sin(1+2*x+3*y)./(2+sin(1+3*x+2*y));
case 56
    ff = @(x,y) exp(1-x.^2-y.^2)./exp(1-x-y);
case 57
    ff = @(x,y) (log(x.^2-y.^3+2)/log(3)).^2;

```

```

case 58
    ff = @(x,y) cos(3*y).^2;
case 59
    ff = @(x,y) ((1+2*x+ 3*y)/6).^7;
case 60
    ff = @(x,y) sin(1+cos(x.^2+y.^2));
case 61
    ff = @(x,y) (cos(1+sin(1+cos(x.^2+y.^2))))).^2;
case 62
    ff = @(x,y) exp(-sin(1+sin(1+sin(x.^2+y.^2))));
case 63
    ff = @(x,y) (sin(sin(sin(sin(sin(sin(x.^2+y.^2)))))))).^3;
case 64
    ff = @(x,y) sin(x+y)./(3+sin(sin(sin(sin(x.^2+y.^2))));
case 65
    ff = @(x,y) sin(2*x.^2+3*y.^3);
case 66
    ff = @(x,y) log(x.^2-y.^3+2)/log(3);
case 67
    ff = @(x,y) exp(1-x.^2-y.^2)/exp(1);
case 68
    ff = @(x,y) sin(x.^2+y.^2);
case 69
    ff = @(x,y) sin(5*x).*sin(4*y);
case 70
    ff = @(x,y) sin(2*x).*sin(3*y);
case 71
    ff = @(x,y) sin(6*x).*sin(7*y);
case 72
    ff = @(x,y) sin(8*x).*sin(8*y);
case 73
    ff = @(x,y) cos(2*(x-y)/pi);
case 74
    ff = @(x,y) max(x-0.5,0);
case 75
    ff = @(x,y) max(x-0.5,0).*max(y-0.5,0);
case 76
    ff = @(x,y) max(x-0.25,0) - max(x-0.75,0);
case 77
    ff = @(x,y) (20*max(x-0.25,0).*max(0.75-x,0)).^2;
case 78
    ff = @(x,y) (20*max(x-0.25,0).*max(0.75-x,0)).^2.*(20*max(y-0.25,0).*max(0.75-y,0)).^2;
case 79
    ff = @(x,y) (100*(max(x-0.2,0).*max(0.8-x,0).*max(y-0.2,0).*max(0.8-y,0))).^2;
case 80
    ff = @(x,y) (x./(1+exp(100*(x-0.25)))+ y./(1+exp(100*(0.75-x)))).* ...
        1./(1+exp(100*(y-0.25)))+ 1./(1+exp(100*(0.75-y))));
case 81
    ff = @(x,y) (max(x-0.25,0).*max(y-0.25,0)).^3;
case 82
    ff = @(x,y) (max(x-0.25,0).*max(0.75-x,0)).^2;
case 83
    ff = @(x,y) (max(x-0.3,0).*max(y-0.3,0)).^2;
case 84

```

```

        ff = @(x,y) tan(x.^2-y.^2)/tan(1);
case 85
    ff = @(x,y) (tan(x-y)).^2;
case 86
    ff = @(x,y) (tan(x-y)).^3;
case 87
    ff = @(x,y) exp(x.^3-y.^2);
case 88
    ff = @(x,y) sin(2*pi*(x+y));
case 89
    ff = @(x,y) log(x.^2-y.^3+2);
case 90
    ff = @(x,y) cos(1./(1+x.*y));
case 91
    ff = @(x,y) cos(2*pi*(x.^2+y.^2));
case 92
    ff = @(x,y) cos(2*pi*(x.^2-y.^2));
case 93
    ff = @(x,y) sin(2*pi*x).*sin(2*pi*y);
case 94
    ff = @(x,y) (x.*(1-x).*y.*(1-y)).^2;
case 95
    ff = @(x,y) (sin(pi*x).*sin(pi*y)).^2;
case 96
    ff = @(x,y) (x.*(1-x).*y.*(1-y));
case 97
    ff = @(x,y) (x.*(1-x).*y.*(1-y)).^4;
case 98
    ff = @(x,y) (sin(pi*x).*sin(pi*y)).^3;
case 99
    ff = @(x,y) (sin(pi*x).*sin(pi*y)).^4;
case 100
    ff = @(x,y) (x.*(1-x).*y.*(1-y)).^8;
end

```

5.2 100 Testing Functions in 3D

```

function ff=testfunctions3d(x,y,z,caseNum)

switch caseNum
case 1
    ff = @(x,y,z) x+ y.^2+z.^2.*y.*x;
case 2
    ff = @(x,y,z) (x.^3+y.^3+z.^3)/(1+y.^2+z.^2);
case 3
    ff = @(x,y,z) 1./(1+x.^2+y.^2+z.^2);
case 4
    ff = @(x,y,z) cos(1./(1+x.*y.*z));
case 5
    ff = @(x,y,z) sin(1+2*x+3*y+z);
case 6
    ff = @(x,y,z) exp(1-x.^2-y.^2-z.^2)/exp(1);
case 7

```

```

ff = @(x,y,z) log(x.^2-y.^3+z.^4+2)/log(3);
case 8
ff = @(x,y,z) tan((x+y+z)/3)/tan(1);
case 9
ff = @(x,y,z) ((1+2*x+ 3*y+4*z)/10).^9;
case 10
ff = @(x,y,z) sin(1+cos(x.^2+y.^2+z.^2));
case 11
ff = @(x,y,z) cos(1+sin(1+cos(x.^2+y.^2+z.^2)));
case 12
ff = @(x,y,z) exp(-cos(1+sin(1+cos(x.^2+y.^2+z.^2))));
case 13
ff = @(x,y,z) sin(sin(sin(sin(sin(x.^2+y.^2))))) );
case 14
ff = @(x,y,z) 1./(3+sin(sin(sin(sin(x.^2-z.^2))))) );
case 15
ff = @(x,y,z) max(x-0.25,0).*max(y-0.25,0).*max(z-0.25,0);
case 16
ff = @(x,y,z) max(x-0.25,0).*max(0.75-x,0);
case 17
ff = @(x,y,z) (max(x-0.3,0).*max(y-0.3,0).*max(z-0.3,0)).^2;
case 18
ff = @(x,y,z) 10*(max(x-0.2,0).*max(0.8-x,0).*max(y-0.2,0).*max(0.8-y,0));
case 19
ff = @(x,y,z) (x.*(1-x).*y.*(1-y).*z.*(1-z));
case 20
ff = @(x,y,z) (x.*(1-x).*y.*(1-y).*z.*(1-z)).^4;
case 21
ff = @(x,y,z) sin(2*x+3*y-4*z);
case 22
ff = @(x,y,z) sin(x.^2-y.^2-z.^2);
case 23
ff = @(x,y,z) cos(x.^2+y.^3+z.^4);
case 24
ff = @(x,y,z) sin(1+cos(x.^2+y.^2+z.^2));
case 25
ff = @(x,y,z) cos(1+sin(1+cos(x.^2-y.^2-2*z)));
case 26
ff = @(x,y,z) exp(-cos(1+sin(1+cos(x.^2-y.*z))));
case 27
ff = @(x,y,z) sin(sin(sin(sin(x.^2-y.^2.*z.^2))));
case 28
ff = @(x,y,z) sin(sin(sin(sin(sin(x.^2-y.^2+z.^2))))) );
case 29
ff = @(x,y,z) sin(sin(sin(sin(sin(sin(x.^2+y.*z))))) );
case 30
ff = @(x,y,z) 1./(3+sin(sin(sin(sin(x.^2+y.*z))))) );
case 31
ff = @(x,y,z) cos(5*x).*cos(4*y).*cos(3*z);
case 32
ff = @(x,y,z) sin(pi*x.*y.*z).^2;
case 33
ff = @(x,y,z) tan(x).*tan(y).*tan(z);
case 34

```

```

ff = @(x,y,z) tan(x/2).*tan(y/2).*tan(z/2);
case 35
ff = @(x,y,z) (x-2*y.*z).*sin(2*x-y.*z);
case 36
ff = @(x,y,z) asin(x).*asin(2*(y-0.5)).*asin(3*(z-0.5)/2);
case 37
ff = @(x,y,z) (x.^2-y.^2)./(1+sin(x).^2+sin(y).^2+sin(z).^2);
case 38
ff = @(x,y,z) cos(x.^2-y.^2)./(1+x.^2+y.^3+z.^4);
case 39
ff = @(x,y,z) sin(1+cos(x.^2-y.*z))./(1+cos(pi*x/2));
case 40
ff = @(x,y,z) sin(1+log(1+x.^2+y.^2+z.^2));
case 41
ff = @(x,y,z) log(1+x.^2+y.^2+z.^2)/log(3);
case 42
ff = @(x,y,z) x.*y.*z.*exp(1-(x.^2+y.^2+z.^2)/3);
case 43
ff = @(x,y,z) x.*y.*log(1+x.^2+y.^2+z.^2);
case 44
ff = @(x,y,z) x.*y.*z.*log(1+x.^2+y.^2+z.^2);
case 45
ff = @(x,y,z) (x.^2+y.^2+z.^2).*exp(1-x.^2-y.^2-z.^2);
case 46
ff = @(x,y,z) x.*y.*log(1+x.^2+y.^2+z.^2).*sin(pi*x+y+z);
case 47
ff = @(x,y,z) sin(x+y+z).*log(1+x.^2+y.^2+z.^2);
case 48
ff = @(x,y,z) log(x.^2-y.^3+2*x.*z)/log(3);
case 49
ff = @(x,y,z) (log(5+ x.^3+z))./log(3+y.^2);
case 50
ff = @(x,y,z) log(1+x.^2+y.^2+z.^2)./(1+x.^2+y.^2);
case 51
ff = @(x,y,z) (x.*z+ y.^2).^2./(3+sin(x.*z+y.^2));
case 52
ff = @(x,y,z) sin(x.*z).^3./(3+sin(y).^2);
case 53
ff = @(x,y,z) sin(x+y+z)./(1+x.^2+y.^2+z.^2);
case 54
ff = @(x,y,z) cos(x.^2+y.^2+1)./(1+x.*y.*z));
case 55
ff = @(x,y,z) sin(1+2*x+3*y+4*z)./(2+sin(1+3*x+2*y));
case 56
ff = @(x,y,z) exp(1-x.^2-y.^2-z.^2)./exp(1-x-y-z);
case 57
ff = @(x,y,z) (log(x.*y.*z+3)/log(3)).^2;
case 58
ff = @(x,y,z) cos(3*y.*z.*x).^2;
case 59
ff = @(x,y,z) ((1+2*x+ 3*y+4*z)/9).^7;
case 60
ff = @(x,y,z) sin(1+cos(x.^2+y.^2+z.^2));
case 61

```



```

ff = @(x,y,z) (cos(1+sin(1+cos(x.^2+y.^2+z.^2))))).^2;
case 62
ff = @(x,y,z) exp(-sin(1+sin(1+sin(x.^2+y.^2+z.^2))));
case 63
ff = @(x,y,z) (sin(sin(sin(sin(sin(sin(x.^2+y.^2+z.^2)))))))).^3;
case 64
ff = @(x,y,z) sin(x+y+z)/(3+sin(sin(sin(sin(x.^2+y.^2))));
case 65
ff = @(x,y,z) sin(2*x.^2+y.^3-z.^4);
case 66
ff = @(x,y,z) log(x.^2-sin(y).^3+3*cos(z).^2)/log(3);
case 67
ff = @(x,y,z) exp(3-sin(x).^2-sin(y).^2-sin(z).^2);
case 68
ff = @(x,y,z) sin(x.^2+y.^2+z.^2);
case 69
ff = @(x,y,z) (x.*(1-x).*y.*(1-y).(1-z).(1+z)).^2;
case 70
ff = @(x,y,z) sin(2*x).*sin(3*y).*sin(4*z);
case 71
ff = @(x,y,z) sin(6*x).*sin(4*y).*sin(5*z);
case 72
ff = @(x,y,z) sin(4*x).*sin(4*y).*sin(4*z);
case 73
ff = @(x,y,z) max(x-0.5,0)+max(y-0.5,0)+max(z-0.5,0);
case 74
ff = @(x,y,z) max(x-0.5,0).*max(y-0.5,0).*max(z-0.5,0);
case 75
ff = @(x,y,z) (max(x-0.25,0) - max(x-0.75,0)).*(max(y-0.25,0) - max(y-0.75,0)).* ...
(max(z-0.25,0) - max(z-0.75,0));
case 76
ff = @(x,y,z) (10*max(x-0.25,0).*max(0.75-x,0)).^2;
case 77
ff = @(x,y,z) (10*max(x-0.25,0).*max(0.75-x,0)).^2.*(20*max(y-0.25,0).*max(0.75-y,0)).^2;
case 78
ff = @(x,y,z) (10*(max(x-0.2,0).*max(0.8-x,0).*max(y-0.2,0).*max(0.8-y,0))).^2;
case 79
ff = @(x,y,z) cos(2*pi*x).*cos(2*pi*y).*cos(2*pi*z);
case 80
ff = @(x,y,z) (sin(pi*x).*sin(pi*y).*cos(pi*z)).^3;
case 81
ff = @(x,y,z) (sin(pi*x).*sin(pi*y).*sin(pi*z)).^4;
case 82
ff = @(x,y,z) (x.*(1-x).*y.*(1-y).*z.*(1-z)).^8;
case 83
ff = @(x,y,z) asin(x).*asin(y).*asin(z);
case 84
ff = @(x,y,z) ((asin(x).*asin(y).*asin(z))/4).^3;
case 85
ff = @(x,y,z) ((asin(x)+ 2*asin(y)+3*asin(z))/6).^4;
case 86
ff = @(x,y,z) (atan(10*x)+atan(5*y)+atan(3*z));
case 87
ff = @(x,y,z) ((acos(x).*acos(y).*acos(z))/4).^3;

```

```

case 88
    ff = @(x,y,z) sin(asin(x)).*cos(2*acos(y)).*sin(3*acos(z));
case 89
    ff = @(x,y,z) ((1+2*sin(x)+3*cos(y)+4*tan(z))/10).^4;
case 90
    ff = @(x,y,z) (x+y.*z)./(5+asin(x).*asin(y).*asin(z));
case 91
    ff = @(x,y,z) (x./(1+exp(100*(x-0.25))) + y./(1+exp(100*(0.75-x)))).* ...
        (1./(1+exp(100*(y-0.25))) + 1./(1+exp(100*(0.75-y))));
case 92
    ff = @(x,y,z) (max(x-0.25,0).*max(y-0.25,0).*max(z-0.2,0)).^3;
case 93
    ff = @(x,y,z) (max(x-0.25,0).*max(0.75-x,0).*max(y-0.25,0).*max(0.75-y,0).* ...
        max(z-0.25,0).*max(0.75-z,0)).^2;
case 94
    ff = @(x,y,z) (max(x-0.3,0).*max(y-0.3,0).*max(z-0.2,0)).^2;
case 95
    ff = @(x,y,z) tan(x.^2-y.^2)/tan(1);
case 96
    ff = @(x,y,z) (tan(x-y/2-z/2)).^2;
case 97
    ff = @(x,y,z) (tan((x+y+z)/3)).^3;
case 98
    ff = @(x,y,z) ((1+2*x+3*y+4*z)/8).^4;
case 99
    ff = @(x,y,z) sin(2*pi*(x.^2+y.^2+z.^2));
case 100
    ff = @(x,y,z) sin(5*x).*sin(4*y).*sin(3*z);
end

```

5.3 One of Our Main Driving Codes

```

%This is a demo code for using cubic LKB splines to approximate smooth global functions.
%It is based on LKB-splines which are obtained by replacing the K-outer function
% by cubic B-splines to have KB splines and then by denoising the KB splines.
% K-outer functions are from the Kolmogorov representation theorem.
% This demo code is written by Dr. Ming-Jun Lai based on the 2D KST
% construction from Zhaiming Shen who is a Ph.D. student under Dr. Ming-Jun Lai's
% supervision in 2018--2023.
% The first part of the demo is to generate the KB and LKB splines.
% Then the code is divided into two parts for two data fitting strategies.
% The first strategy is to solve a discrete least squares fit of various functions based
% on 101x101 equally-spaced points over [0, 1]^2 and the function values.
% The second strategy is to generate a set of magic locations with the set containing
% much less than 101x101 points. Based on the magic data locations, we solve the
% discrete least squares fit for the same testing functions in the first strategy.
% Finally we compare the accuracies of LKB spline approximation of various testing
% functions based on 101x101 points vs based the magic set.
% The comparison shows that the accuracies are similar, the ratios of the
% accuracies from two strategies are between 1 to 3.

```

```

% The following line is the beginning of this demo code.
phi_q;%you can comment off phi_q after the first run

% number n of linear spline basis and n = length(LKB)
n = 21; M=100;

%We first generate cubic KB splines
KB=CubicKBsplines(n,Lambda,phi_0,phi_1,phi_2,phi_3,phi_4);

% number of data locations over [0, 1]^2. %hh = 1/(length(LKB{1})-1); %%
hh = 0.01; xx = linspace(0,1,1/hh+1);yy = linspace(0,1,1/hh+1);
[xx,yy] = meshgrid(xx,yy);
LaisSplines4denoising %this generates cubic LKB splines and save them in LKB and LKB2.

%The discrete least squares matrix based on 101x101 equally-spaced
%points over [0, 1]^2.
X_data = zeros((1/hh+1)^2, n);
for i = 1:n
    X_data(:,i) = reshape(LKB{i}, [],1);
end

hhh = 0.0025; %We will use this set of points for evaluation.
xxx = linspace(0,1,1/hhh+1);yyy = linspace(0,1,1/hhh+1);
[xxx,yyy] = meshgrid(xxx,yyy);

%strategy 1, we use a compressive sensing approach to find the sparse solution.
KBCS=zeros(M,5); %error matrix.
Phi=X_data; Phi=full(Phi); %err=1e-4;
I=isnan(Phi); J=find(I==1); Phi(J)=0;
[m,L]=size(Phi); A=zeros(L,1); NN=zeros(30,1);
for i=1:L
    a=norm(Phi(:,i)); Phi(:,i)=Phi(:,i)/a; %normalization
    A(i)=a;
end
I=isnan(Phi); J=find(I==1); Phi(J)=0;
for k=1:M
ny=testfunctions_2d(xx,yy,k);
y_LS = reshape(ny(xx,yy), [],1);
x0= myOMP(Phi,y_LS,500); norm(Phi*x0-y_LS,inf);
I=find(abs(x0)>=1e-8); [L, size(I)], NN(k)=size(I,1);
coeff=zeros(L,1); coeff(I)=x0(I)./A(I); %coeff to be sent via internet.
f_reconst = 0;
for i =1:n
    f_reconst = f_reconst + coeff(i)*LKB2{i};
end
spVal = SplineEvaluation2D(V,T,Analyze,f_reconst, d, xxx(:), yyy(:), tol);
exact=ny(xxx,yyy);
%figure, subplot(131), SplV=reshape(spVal,401,401); surf(xxx,yyy,SplV), shading interp

```

```

%subplot(132), surf(xxx,yyy,exact), shading interp
%subplot(133), surf(xxx,yyy,exact-SplV), shading interp
RMSE=rms((exact(:)-spVal(:))./max(1,abs(exact(:))));
Rel_L2_error = norm(exact(:)-spVal(:))/norm(exact(:));
Linf=norm(exact(:)-spVal(:),inf)/norm(exact(:),inf);
KBCS(k,:)= [k,RMSE,Rel_L2_error,Linf NN(k)];
end

%strategy 2: We first find a magic point set.
Phi=X_data; Phi=full(Phi); err=1e-4;
I=isnan(Phi); J=find(I==1); Phi(J)=0;
[m,L]=size(Phi); A=zeros(L,1); NNr=zeros(20,1);
for i=1:L
    a(i)=norm(Phi(:,i));
end
Iind=find(abs(a)>=1e-6);
nPhi=Phi(:,Iind); [n1,r]=size(nPhi);

%The following computation is based on a matrix cross approximation.
Im=LaisCrossApproximation(nPhi);
%figure, plot(xx(Im),yy(Im),'r*')
%title('The magic locations for data fitting based on KST')
nPhi2=nPhi(Im,:);
NNr=ones(M,1); NP=size(Im',1);
KBSME=zeros(M,4);
for k=1:M
ny=testfunctions_2d(xx,yy,k);
y_LS = reshape(ny(xx(Im),yy(Im)), [],1);
x0=myOMP(nPhi2,y_LS,500);
coeff=zeros(L,1); coeff(Iind)=x0;
I=find(abs(coeff)>=1e-8);NNr(k)=size(I,1);
f_reconst = 0;
for i =1:n
    f_reconst = f_reconst + coeff(i)*LKB2{i};
end
spVal = SplineEvaluation2D(V,T,Analyze,f_reconst, d, xxx(:), yyy(:), tol);
exact=ny(xxx,yyy);
%figure, subplot(131), SplV=reshape(spVal,401,401); surf(xxx,yyy,SplV), shading interp
%subplot(132), surf(xxx,yyy,exact), shading interp
%subplot(133), surf(xxx,yyy,exact-SplV), shading interp
RMSE=rms((exact(:)-spVal(:))./max(1,abs(exact(:))));
Rel_L2_error = norm(exact(:)-spVal)/norm(exact(:));
Linf=norm(exact(:)-spVal,inf)/norm(exact(:),inf);
KBSME(k,:)= [k,RMSE,Rel_L2_error,Linf];
end
%Plot the computational results.
M=100;
b1=KBSME(1:M,2);c1=KBCS(1:M,2);

```

```
figure, subplot(121), plot(xx(Im),yy(Im),'r*'), grid on
title('A Set of Magic Data Locations')
subplot(122), hold on,plot(c1,'r'), plot(b1,'b'),
legend('RMSE1012','RMSEmagic'),
title(['RMSEs of DLS from 1012 vs ',num2str(NP), ' points'])
return
```